Journal Pre-proof

Novel phthalide derivatives: synthesis and anti-inflammatory activity in vitro and in vivo

Liu Zeng Chen, Jing Wu, Kang Li, Qian Qian Wu, Rui Chen, Xin Hua Liu, Ban Feng Ruan

PII: S0223-5234(20)30694-2

DOI: https://doi.org/10.1016/j.ejmech.2020.112722

Reference: EJMECH 112722

To appear in: *European Journal of Medicinal Chemistry*

Received Date: 6 July 2020

Revised Date: 31 July 2020

Accepted Date: 2 August 2020

Please cite this article as: L.Z. Chen, J. Wu, K. Li, Q.Q. Wu, R. Chen, X.H. Liu, B.F. Ruan, Novel phthalide derivatives: synthesis and anti-inflammatory activity in vitro and in vivo, *European Journal of Medicinal Chemistry*, https://doi.org/10.1016/j.ejmech.2020.112722.

Novel phthalide derivatives: synthesis and anti-inflammatory activity *in vitro* and *in vivo*

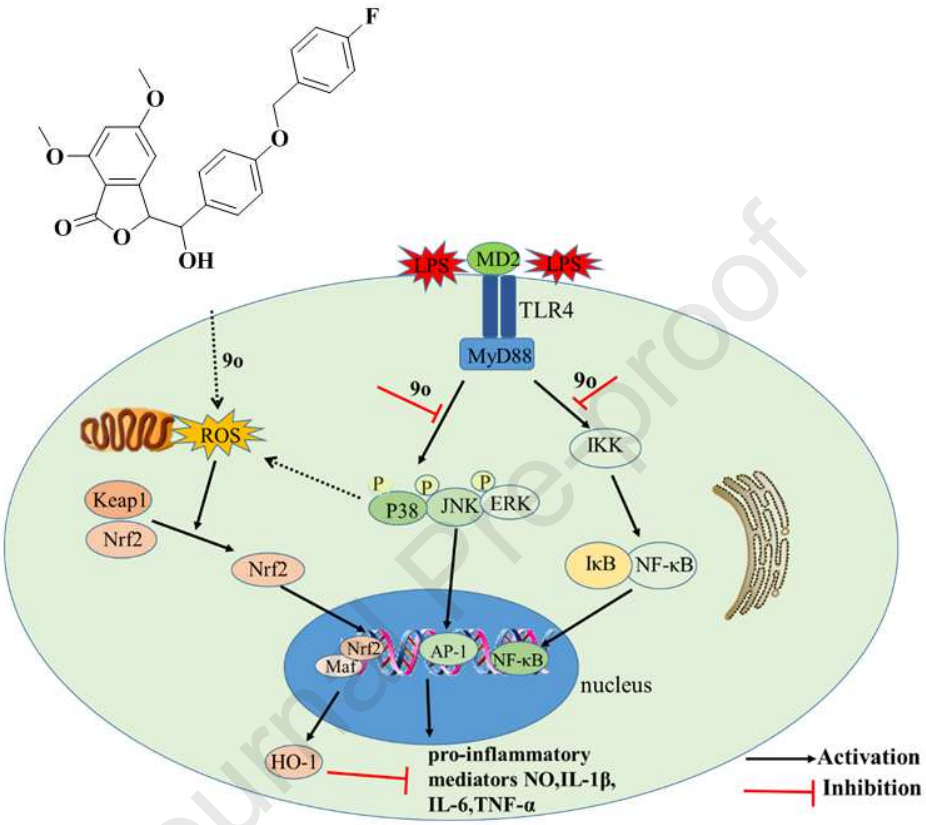

Thirty-one novel phthalide derivatives were synthesized and evaluated to discover novel agents with anti-inflammatory activity. Among them, compound **9o** was the most one with potent NO inhibitory activity and without obvious cytotoxicity. The preliminary mechanism of anti-inflammatory activity was revealed. The further in *vivo* anti-inflammatory studies showed that this title compound had a good therapeutic effect against AIA rats.

Novel phthalide derivatives: synthesis and anti-inflammatory activity *in vitro* and *in vivo*

Liu Zeng Chen[a], Jing Wu[a], Kang Li[a], Qian Qian Wu[a], Rui Chen[a], Xin Hua Liu[a,*], Ban Feng Ruan*[,b]

[a] *School of Pharmacy, Anhui Medical University, Hefei, 230032, P. R. China*

[b] *Key Lab of Biofabrication of Anhui Higher Education, Hefei University, Hefei 230601, P. R. China*

Abstract: Phthalide is a promising chemical scaffold and has been proved to show potent anti-inflammatory efficacy. In this study, three series, total of 31 novel phthalide derivatives were designed and synthesized, their anti-inflammatory activities were screened in *vitro* and in *vivo*. The anti-inflammatory activity of all the compounds were screened on LPS induced NO production to evaluating their inhibitory effects. Structure-activity relationship has been concluded, and finally 3-((4-((4-fluorobenzyl)oxy)phenyl)(hydroxy)methyl)-5,7-dimethoxyisobenzofuran-1(3H)-one (compound **9o)** was found to be the active one with low toxicity, which showed 95.23% inhibitory rate at 10 μM with IC_{50} value of 0.76 μM against LPS-induced NO over expression. Preliminary mechanism studies indicated that compound **9o** activated Nrf2/HO-1 signalling pathway via accumulation ROS and blocks the NF-κB/MAPK signaling pathway. The *in vivo* anti-inflammatory activity shown that compound **9o** had obvious therapeutic effect against the adjuvant-induced rat arthritis model.

Keywords: Phthalide derivatives; design; synthesis; anti-inflammatory

---

*Corresponding author, E-mail: xhliuhx@163.com (Xin Hua Liu).
ruanbf@hfuu.edu.cn (Ban Feng Ruan).

1. Introduction

Inflammation is a series of complex defense-related reactions caused by invading microbes or physical injuries [1]. In the innate immune response, macrophages mediate most of the inflammatory cellular and molecular pathophysiology by producing various pro-inflammatory mediators, and play an important role in promoting cellular repair and protection [2-4]. Unregulated production of these pro-inflammatory mediators such as nitric oxide (NO), interleukin-6 (IL-6), tumor necrosis factor-α (TNF-α), interleukin-1β (IL-1β) and interleukin-12 which can lead to wide range of diseases, including rheumatoid arthritis, sepsis and inflammatory bowel disease[5,6]. Therefore, there is an urgent need to find effective drugs or therapies that can inhibit the production and release of pro-inflammatory cytokines.

Toll-like receptors are transmembrane proteins of pattern recognition receptors of lipopolysaccharide (LPS) [7]. It controls the initial inflammatory response and plays an important role in innate immune system[8]. The complex formed by LPS and TLR4 leads to the activation of intracellular signaling pathway [9]. The pathway mediates the activation of IκB kinases, p38, c-Jun NH2-terminal kinase (JNK) and (ERK)-1/2 mitogen-activated protein kinases (MAPKs), leading to activation of transcription factors nuclear factor-κB (NF-κB) and AP-1 enter the nucleus[10, 11]. The nuclear factor erythroid 2-related factor 2 (Nrf2) is a key and important transcription factor, which contributes to anti-inflammatory processes and regulates the expressions of a series of antioxidant enzymes [12, 13]. In macrophages, Nrf2 can inhibit the inflammatory response by blocking the transcription of pro-inflammatory cytokines [14]. The activation of Nrf2 activation and regulation of HO-1 are considered to be the main anti-inflammatory and cytoprotective enzymes [15, 16]. Therefore, targeting Nrf2/HO-1 pathway may be a promising strategy for the treatment of inflammatory diseases [17].

Butylphthalide (NBP) is a phthalide extracted from *Angelicae Sinensis Radix*, which is one of the most important traditional Chinese medicines (TCM). Due to its effects on protecting nerve cells, antioxidation and improving brain circulation, the racemic 3-*n*-butylphthalide has been approved by the SFDA of China as a new drug

mainly for the treatment of ischemic stroke since 2002. It is well-known that NBP can inhibit platelet aggregation and thrombosis, improve microcirculation, and reduce brain infarct volume, thus benefiting patients with ischemic stroke[18]. Besides NBP, some other natural phthalides have been shown to active against ischemic stroke-induced brain injury.

Previous studies show that NBP and its derivatives can suppress the inflammatory response caused by cerebral ischemia, which is related to the inhibition of NF-κB signaling pathway (Figure 1). Zou *et al* have investigated the effects of a phthalide derivative CD21 on ischemic brain injury. The results suggest that the anti-stroke of CD21 appear to be mediated partially via the induction of MSR1-promoted DAMP (PRX1) clearance, TLR4/nuclear factor-κB pathway inhibition, and the resolution of inflammation [19]. Several groups have determined that (*Z*)-Ligustilide, another natural compound with phthalide skeleton, can exert anti-inflammatory effects by regulating the NF-κB, MAPK pathways, or by regulating the AP-1 and HO-1 [20-24]. Among them, Guo *et al* found that Levistilide A, a phthalide dimer isolated from *Ligusticum chuanxiong* and *Angelica sinensis* could suppress NLRP3 gene expression by blocking the Syk-p38/JNK pathway [25]. Lee *et al* also found that Cnidilide, an alkylphthalide isolated the roots of *Cnidium officinale*, could suppress LPS-induced NO, PGE2, IL-1β, IL-6 and TNF-α production by AP-1 and MF-κB inactivation in RAW 264.7 macrophages [26]. Therefore, phthalide is a promising chemical scaffold to discovery new anti-inflammatory drugs.

Figure 1

Herein three series of phthalide derivatives were designed and synthesized through above finding. The first one is hybrids of phthalide and 1,2,4-oxadiazole core, inspired by the anti-inflammatory activity of some compounds with 1,2,4-oxadiazole moiety (**Series A)**. In order to investigate the effects of hydrophobic interaction and steric configuration, the second series of 3-hydroxy-benzhydrolphthalides (**Series B)** were synthesized. Based on the activity of (*Z*)-Ligustilide, the third one, a series of

(*Z*)-3-benzylidene-phthalides by eliminating the chiral hydroxy group of series B (**Series C**) were constructed at last (Figure 2). On the basis of balancing anti-inflammatory activity and toxicity, the title phthalide derivative was used to explore ameliorate inflammation in a CFA-induced arthritis (AIA) mouse model.

Figure 2

2. Results and discussion

2.1 Chemistry

The synthesis of the first series of derivatives with 1,2,4- oxadiazole moiety (**5a**~**5e**) was outlined in Scheme 1. Compounds (**3a**~**3e**) were obtained by reacting different nitriles with hydroxylamine hydrochloride in the presence of triethylamine in methanol under reflux. Amide coupling of the respective oximes with phthalide-3-acetic acid (**4**), following by subsequent cyclization and afforded the title compounds **5a**~**5e**.

Scheme 1

The synthesis of the second series of phthalide derivatives was exhibited in Scheme 2. Actually, this series of compounds are by-products of Pinnick oxidation. At first, we wanted to convert the aldehyde group of **8b**, a derivative of resveratrol, to the corresponding carboxyl group. When the reaction was carried out at 0 °C, the main product was the carboxylic acid [27]. However, when the reaction temperature went up to 50 °C, a new main product was obtained with good yield. After characterized by NMR, MS and the X-ray single crystal diffraction, we found that a new phthalide derivative was synthesized (**9b**) in the single-step reaction. The possible mechanism of this reaction was proposed and outlined in Figure 3.

Scheme 2

Figure 3

To understand the influence of the chirality of the second series of compounds, the hydroxy groups of compounds **9b**, **9n** and **9o** were eliminated to afford the corresponding 3-benzylidenephthalides (**10b**, **10n** and **10o**) Scheme 3 [28]. The double bond of **10b**, **10n** and **10o** were found to be (*Z*)-configuration. This was indicated by δ_H of the vinyl protons of **10b**, **10n** and **10o** (δ 6.31, 6.32 and 6.29 ppm, respectively) because the chemical shifts of the vinyl protons of unstable (*E*)-isomers of 3-benzylidenephtha-lides are shifted downfield from the corresponding stable (*Z*)-isomers [29].

Scheme 3

*2.2 Crystal structure of compound **9b***

The structure of compound **9b** was determined by X-ray crystallography (Figure 4). Crystallographical data: Crystallographic data: $C_{18}H_{18}O_6$, Triclinic, space group P_{-1}; a = 9.635(2), b = 9.956(2), c = 10.257(2) (Å); α = 65.318(2), β = 68.283(2), γ = 68.615(2) (°), V = 804.4(3) nm^3, T = 298 (2) K, Z = 2, Dc = 1.364 g/cm^3, $F(000)$ = 348, Reflections collected/unique = 5506/2223, Data/restraints/parameters = 2808/0/221, Goodness of fit on F^2 = 1.082, Fine, R_1 = 0.053, $wR(F^2)$ = 0.1448. Crystallographic data (excluding structure factors) for the structures have been deposited into the Cambridge Crystallographic Data Center (CCDC no: 844477).

Figure 4

2.3 Anti-inflammatory activity of compounds

Firstly, we determined the intrinsic cytotoxicity of the title compounds against RAW264.7 cells by MTT assay, and found that the target compounds displayed low intrinsic cytotoxicity. As shown in Figure 5 (A and B). All compounds showed no significant intrinsic cytotoxicity at 20 μM. Subsequently, the anti-inflammatory activity of all compounds were determined according to the previous method [30], and LPS stimulated RAW264.7 cells as an evaluation model. Excessive NO

production has been found to play an important role in many inflammatory diseases[31]. Here, all compounds were tested for their ability to inhibit NO overexpression. Griess reagent was used to determine the concentration of NO in cell supernatant. As shown in Figure 5 (C and D) the screening results showed that most of the compounds could reduce the LPS-induced NO secretion at a dose of 10 μM. It is noteworthy that most compounds exhibited stronger inhibition of NO production compared with the references Celecoxib and Indomethacin. Therefore, these compounds are valuable for further evaluation.

Figure 5

2.4 Inhibitory effect of NO production and expression of pro-inflammatory mediators

Different concentrations (0.625, 1.25, 2.5, 5, 10 μM) of compounds were selected for further study. Compounds dose-dependently inhibited NO production in LPS-stimulated RAW264.7 cells (Table 1). On the whole, the toxicity of all compounds, lower than 40 μM, which were acceptable. The structure-activity relationships of the three series against NO inhibitory activity were clear. Compounds **5a**~**5e** (**Series A**) had no obvious inhibitory activity against NO, IR is less than 25% and with IC_{50} › 10 μM. After hydroxymethylation optimization (**Series B,** compounds **9a**~**9v**), which significantly improve the inhibitory activity against NO, among them the IR values of compounds **9e**, **9f**, **9i**, **9o**, **9p**, **9q**, **9R**, **9t** and **9u** (62.24~95.23%) are better than that of Indomethacin (61.59%); the IC_{50} (NO) values of above compounds ranging from 0.76 to 10 μM), which also surpassing of Indomethacin. What's more, the IC_{50s} of compounds **9e**, **9i**, **9m** and **9o** is lower than 2.0 μM, which show strong activity against NO, among this series, benzyl substitution is the best, such as compound **9o**.

Unfortunately, the design based on (*Z*)-ligustilide failed. Compounds **10b**, **10n** and **10o** (**Series C**) exhibited inhibitory activity against NO ranging of 36%~48%, which was significantly worse than that of **Series B**.

It is interesting, title compound **9o** could significantly decreased production of NO with IC_{50} values of 0.76 μM. At the same time, the IC_{50} value of compound **9o** cytotoxicity exceeds 40 μM. In addition, the inhibitory effect of compound **9o** on pro-inflammatory mediators iNOS and COX-2 expression were analyzed by Western blot. Treatment of RAW264.7 cells with compound **9o** decreased the LPS-induced expression levels of iNOS and COX-2 in a concentration-dependent manner (Figure 6). These results prove that compound **9o** prevents LPS-induced expression of inflammatory mediators. So, it is worthy of further study.

Table 1

Figure 6

*2.5 Effect of compound **9o** on the intracellular ROS generation*

Previous studies have shown that the increase of ROS is related to the activation of inflammation[32]. On this basis, we investigated the effect of compound **9o** on ROS production by analyzing the fluorescence intensity of DCF-DA. As expected, LPS stimulated ROS accumulation compared with untreated cells. Interestingly, ROS production was significantly increased in a concentration dependent manner in the compound **9o** (0.5, 1 and 2 μM). The results showed that compound **9o** could not inhibit ROS production in LPS-pretreated RAW264.7 cells (Figure 7).

Figure 7

*2.6 Compound **9o** activates Nrf2/HO-1 pathway via ROS*

ROS are products of normal cell metabolism [33]. Accumulation ROS may destroy the balance between antioxidant and pro-oxidant systems, and then activate various defense mechanisms in cells [33, 34]. Cumulative evidence suggests that ROS has an important effect on Nrf2 activation [35]. Nrf2 is considered to be a key transcription factor for cell homeostasis, and it has been confirmed that Nrf2 has antioxidant and anti-inflammatory effects by interacting with various signaling

pathways[36]. To investigate the anti-inflammatory mechanisms of compound **9o**, we further determined whether compound **9o** activated Nrf2/HO-1 signaling pathway in RAW264.7 cells. The effect of compound **9o** on Nrf2 / HO-1 signal pathway was studied by Western blot. As we expected, compound **9o** treatment significantly increased Nrf2 protein expression in the nucleus and HO-1 protein expression in RAW264.7 cells (Figure 8A). At the same time, the localization of nuclear factor Nrf2 in RAW264.7 cells was examined by immunofluorescence. As shown in the Figure 8B, Nrf2 was obviously transferred to the nucleus after compound **9o** treatment, and the higher compound **9o** concentration, the more obvious Nrf2 nuclear transfer. These results indicated that compound **9o**-mediated Nrf2/HO-1 pathway activation. To verify whether ROS is involved in the activation of the Nrf2/HO-1 pathway by compound **9o**. NO production in RAW264.7 cells co-treated with compound **9o** and NAC (ROS scavenger) were examined. Moreover, NAC significantly reversed compound **9o**-mediated suppression of NO production in LPS-stimulated RAW264.7 cells (Figure 8C), suggesting that compound **9o** may exert anti-inflammatory effects by activates Nrf2/HO-1 pathway via accumulation ROS. From Figure 8C, we found that although NAC reversed the inhibitory effect of compound **9o** on NO production, compound **9o** still had a certain ability to inhibit NO secretion. So we think that this compound can also exert anti-inflammatory activity through other pathways.

Figure 8

*2.7 Compound **9o** inhibits LPS-induced activation of NF-κB and MAPKs*

Activating Nrf2 can suppress activation of NF-κB signaling pathway [37, 38]. In addition, inhibition of NF-κB and MAPKs signaling activation is considered to be an important target for the development of anti-inflammatory drugs [39]. Thus, we examined whether compound **9o** suppressed LPS-induced activation of NF-κB and MAPKs. Here, we analyzed it by Western blotting. The results showed compound **9o** inhibited LPS-induced degradation and resynthesis of IκB protein. Meanwhile it could effect of p65 phosphorylation and inhibit NF-κB p65 translocate into the nucleus

(Figure 9A). We examined the effect of compound **9o** on LPS-mediated MAPK signal activation with phosphorylated antibodies. As we expected, compound **9o** time-dependently blocked LPS-induced ERK phosphorylation, JNK phosphorylation and p38 phosphorylation (Figure 9B). These findings demonstrated that this compound blocked NF-κB and MAPKs signaling activation.

Figure 9

2.8 *In vivo activity of compound **9o***

Rheumatoid arthritis (RA) is a chronic inflammatory autoimmune disease characterized by joint swelling, synovitis, and progressive joint injury of cartilage and bone [40]. The complete Freund's adjuvant (CFA)-induced arthritis (AA) is widely used model to study RA because of its similar pathogenesis [41]. Male SD rats, weighing 140-160 g, were randomly divided into groups with 10 rats in each group. CFA consists of in-complete Freund's adjuvant and inactivated BCG vaccine (10 mg/mL). Rat was induced by a single intradermal injection of 0.1 mL CFA and saline (0.9% sodium chloride, as normal) into the right hind paw. After 2 weeks, we observed that 70-80% of the rats showed obvious swelling of the left hind paw, pathological nodules in the tail and ears, and the weight gain of the rats was slowed down and part of the weight was lost. From the 14th day to the 28th day, all experimental group AIA rats were given intragastric administration of different concentrations compound **9o** (20 mg/kg, 40 mg/kg) and Sinomenine (60 mg/kg) once a day. All rats measured the left hind swelling level and weight change every three days. The results were shown in Figure 10A and B), We observed that compound **9o** attenuate paw swelling and weight loss in rats. Histopathological analysis of the ankle joints was performed at the end of the experiment to assess the level of inflammation and tissue changes. The representative histological photos of the tissue sections were shown in the Figure 10C. Compared with normal rats, AIA rats showed extensive inflammatory cell infiltration, synovial hyperplasia and cartilage destruction (Figure 10C normal). AA rats treated with compound **9o** (20 mg/kg) showed moderate

synovial hyperplasia, inflammatory cell infiltration and cartilage destruction (Figure 10 C, **9o** L). Compound **9o** (40 mg/kg) ameliorated cartilage destruction and inflammatory cell infiltration (Figure 10C, **9o** H). Sinomenine (60 mg/kg) showed moderate synovial hyperplasia and keep intact joint cavity. In conclusion, the results indicate that compound **9o** has an anti-inflammatory effect on AA rats.

Figure 10

3. Conclusion

In summary, thirty-one novel phthalide derivatives were synthesized and evaluated to discover novel agents with anti-inflammatory activity. The preliminary screening results indicated that most of the title compounds exhibited potent anti-inflammatory activity. Among them, compound **9o** was the active one with potent NO inhibitory activity and without obvious cytotoxicity. Taken together, compound **9o** showed anti-inflammatory activity through the regulation of three signalling pathways (Figure 11). First, compound **9o** activated Nrf2/HO-1 signalling pathway via accumulation ROS. Second, compound **9o** inhibited NF-κB signalling activation through blocking IκB-α degradation and subsequent p65 nuclear accumulation. Finally, compound **9o** inhibited MAPKs signalling activation through blocking the phosphorylation of ERK1/2, JNK and p38. The further in *vivo* anti-inflammatory studies showed that this compound had a good therapeutic effect on AIA rats. These findings suggest that this title compound may has great potential in the development of anti AA drug.

Figure 11

4. Experimental section

4.1. Chemistry general

All the reagents, solvent, and other chemicals were commercially available from

Aladdin, Adamas, Tan soole *et al*. without further purification. Reactions were monitored by TLC using Silica Gel GF254 precoated plates, and compounds were visualized under UV light (λ = 254 or 365 nm). Column chromatography was performed using silica gel 60 (40–60 μm). ^{1}H and ^{13}C NMR spectra were recorded on a Bruker Avance III 400 MHz spectrometer or an Agilent 600 MHz spectrometer. The NMR solvents were purchased from Sigma-Aldrich (China). Chemical shifts (δ, ppm) are reported relative to the solvent peak ($CDCl_3$): 7.26 [^{1}H] or 77.16 [^{13}C]; DMSO d_6: 2.50 [^{1}H] or 39.52 [^{13}C]). Proton resonances are annotated as: chemical shift (δ), multiplicity (br, broad; s, singlet; d, doublet; m, multiplet), coupling constant (J, Hz), and the number of protons. The ESI-MS spectra were recorded on a Mariner System 5304 Mass spectrometer. Melting points were determined on a XT4MP apparatus (Taike Corp., Beijing, China), and are uncorrected. All characterized compounds had a purity of >95% as measured by analytical reversed-phase high-performance liquid chromatography (HPLC).

4.2. Crystallographic studies

Compound **9b** was chosen for X-ray diffraction analysis performed on a BRUCKER SMART APEX-CCD diffractometer equipped with a graphite monochromatic MoKa radiation (λ = 0.71073 A) radiation at 293(2) K. A total reflection was collected in the range of $0.97<\theta<26.1^{o}$ by using a ψ-ω scan mode with independent ones, of which $I>2\sigma(I)$ were observed and used in the succeeding refinements. The data set were corrected by SADABS program and the structure were solved by direct methods with SHELXS-97 and refined by full-matrix least-squares method on F^2 with SHELXL-97[30]. The non-hydrogen atoms were refined anisotropically, and the hydrogen atoms were added according to theoretical models. The structures were refined by full-matrix least-squares method on F^2 with SHELXT-97.

*4.3. General procedure A: Synthesis of compounds **5a**~**5e***

A solution of appropriate nitriles (**1a**~**1e**, 5.0 mmol, 1.0 equiv), hydroxylamine hydrochloride (**2**, 6.0 mmol, 1.2 equiv) and Et_3N (6.0 mmol, 1.2 equiv) in methanol

(10 mL) was stirred for 6 h at 60 °C. After completion, the solvent was evaporated under reduced pressure and the crude product (**3a**~**3e**) was used for the next step without purification.

The appropriate oximes (**3a**~**3e**, 5.0 mmol, 1.0 equiv), phthalide-3-acetic acid (**4**, 0.96 g, 5.0 mmol, 1.0 equiv) and CDI (0.81 g, 5.0 mmol, 1.0 equiv) were dissolved in DMF (15 mL). The reaction mixture was stirred at 90 °C overnight. After completion, the solvent was evaporated under reduced pressure. The residue was dissolved in EtOAc, washed twice with water and once with brine. The combined organic layer was dried over Na_2SO_4 and then evaporated under reduced pressure. The product was separated using silica gel column chromatography.

*((3-methyl-1,2,4-oxadiazol-5-yl)methyl)isobenzofuran-1(3H)-one (**5a**).* Yellow waxy solid, Yield: 70.5%. ^{1}H NMR (400 MHz, $CDCl_3$) δ 7.93 (d, J = 8.0 Hz, 1H), 7.71 (t, J = 8.0 Hz, 1H), 7.58 (t, J = 8.0 Hz, 1H), 7.52 (d, J = 8.0 Hz, 1H), 5.91 (t, J = 8.0 Hz, 1H), 3.78 (s, 3H), 2.99-2.87 (m, 2H). ^{13}C NMR (101 MHz, $CDCl_3$) δ 169.8, 148.7, 134.3, 129.6, 125.9, 122.1, 52.2, 39.4. ESI MS (m/z) 230 ($M+H^+$); HRMS (ESI) (m/z) calcd for $C_{12}H_{10}N_2O_3$, 230.2230.

*3-((3-phenyl-1,2,4-oxadiazol-5-yl)methyl)isobenzofuran-1(3H)-one (**5b**).* Yellow waxy solid, Yield: 65.5%. ^{1}H NMR (600 MHz, $CDCl_3$) δ 8.00 (d, J = 6.0 Hz, 2H), 7.88 (d, J = 6.0 Hz, 1H), 7.64 (t, J = 6.0 Hz, 1H), 7.52 (t, J = 6.0 Hz, 1H), 7.47-7.41 (m, 4H), 6.03 (t, J = 6.0 Hz, 1H), 3.56-3.48 (m, 2H). ^{13}C NMR (101 MHz, $CDCl_3$) δ 174.7, 169.5, 168.5, 147.7, 134.6, 131.5, 130.0, 129.0, 127.5, 126.3, 126.1, 126.0, 122.1, 32.4. ESI MS (m/z) 293 ($M+H^+$); HRMS (ESI) (m/z) calcd for $C_{17}H_{13}N_2O_3$, 293.0921, found 293.0920.

*3-((3-benzyl-1,2,4-oxadiazol-5-yl)methyl)isobenzofuran-1(3H)-one (**5c**).* White waxy solid, Yield: 60.5%. ^{1}H NMR (400 MHz, $CDCl_3$) δ 7.88 (d, J = 8.0 Hz, 1H), 7.63 (t, J = 8.0, 1H), 7.54 (t, J = 8.0 Hz, 1H), 7.367.26 (m, 6H), 5.94 (t, J = 8.0 Hz, 1H), 4.09-4.01 (m, 2H), 3.49-3.39 (m, 2H). ^{13}C NMR (101 MHz, $CDCl_3$) δ 174.8, 169.7,

169.4, 147.6, 135.2, 134.4, 129.9, 129.0, 128.8, 127.2, 126.0, 125.9, 122.1, 32.2. ESI MS (m/z) 306 ($M+H^+$); HRMS (ESI) (m/z) calcd for $C_{18}H_{14}N_2O_3$, 306.3210.

3-((3-(4-phenoxyphenyl)-1,2,4-oxadiazol-5-yl)methyl)isobenzofuran-1(3H)-one ***(5d)***. White waxy solid, Yield: 75.8%. ^{1}H NMR (600 MHz, $CDCl_3$) δ 8.01 (d, J = 6.0, 2.0 Hz, 2H), 7.93 (d, J = 6.0 Hz, 1H), 7.68 (t, J = 6.0 Hz, 1H), 7.58 (t, J = 6.0 Hz, 1H), 7.44 (d, 1H), 7.37 (t, J = 6.0 Hz, 2H), 7.17 (t, J = 6.0 Hz,1H), 7.05 (t, J = 6.0 Hz, 4H), 6.05 (t, J = 6.0 Hz, 1H), 3.62-3.52 (m, 2H). ^{13}C NMR (101 MHz, $CDCl_3$) δ 174.6, 169.4, 168.0, 160.4, 156.0, 147.8, 134.5, 130.0, 129.3, 126.1, 124.3, 122.1, 120.9, 119.8, 118.3, 32.3. ESI MS (m/z) 385 ($M+H^+$); HRMS (ESI) (m/z) calcd for $C_{23}H_{16}N_2O_4$, 385.1183, found, 385.1181.

3-((3-([1,1'-biphenyl]-4-yl)-1,2,4-oxadiazol-5-yl)methyl)isobenzofuran-1(3H)-one ***(5e)***. White waxy solid, Yield: 73.6%. ^{1}H NMR (600 MHz, $CDCl_3$) δ 8.13 (d, J = 6.0 Hz, 2H), 7.94 (d, J = 6.0 Hz, 1H), 7.71 (t, J = 6.0 Hz, 3H), 7.63 (d, J = 6.0 Hz, 2H), 7.59 (t, J = 6.0, 1H), 7.47 (t, J = 6.0, 3H), 7.39 (t, J = 6.0 Hz, 1H), 6.08 (t, J = 6.0 Hz, 1H), 3.57 (dt, J = 16.0, 9.4 Hz, 2H). ^{13}C NMR (101 MHz, $CDCl_3$) δ 175.0, 174.1, 169.9, 169.1, 148.0, 147.2, 144.5, 144.0, 143.8, 143.5, 134.4, 134.0, 131.3, 130.1, 129.6, 129.0, 128.33 (s), 128.1, 128.0, 127.7, 127.6, 127.2, 127.1, 126.6, 126.1, 125.9, 33.4. ESI MS (m/z) 368 ($M+H^+$); HRMS (ESI) (m/z) calcd for $C_{23}H_{16}N_2O_3$, 368.3920.

4.4. General procedure B: Synthesis of compounds ***9a-9v***

Compounds **8a-8v** were obtained according to the procedure as described. The appropriate aldehyde compound (**8a-8v**, 2.0 mmol, 1.0 equiv) was dissolved in DMSO and saturated sodium dihydrogenphosphate solution (8.0 mmol, 4.0 equiv) at 0 °C. Saturated sodium chlorite solution (30.0 mmol, 15.0 equiv) was then added dropwise with vigorous stirring, and the reaction mixture was stirred at 50 °C for 6 h. When TLC indicated complete consumption of the starting material, the resulting mixture was extracted with EtOAc (×3), and the organic layers were combined dried over Na_2SO_4. After the solvent was evaporated, the product was separated using silica

gel column chromatography.

3-(hydroxy(4-hydroxyphenyl)methyl)-5,7-dimethoxyisobenzofuran-1(3H)-one ***(9a)***. White waxy solid, Yield: 62.6%. ^{1}H NMR (400 MHz, DMSO-d_6) δ 9.32 (s, 1H), 7.13 (d, J = 8.0 Hz, 2H), 6.69 (d, J = 8.0 Hz, 2H), 6.54 (s, 1H), 6.23 (s, 1H), 5.79 (d, J = 4.0 Hz, 1H), 5.51 (d, J = 4.0 Hz, 1H), 4.92(t, J = 4.0 Hz, 1H), 3.82 (s, 3H), 3.78 (s, 3H).^{13}C NMR (101 MHz, DMSO-d_6) δ 167.6, 165.9, 159.2, 157.1, 152.3, 130.6, 128.6, 115.0, 107.1, 100.3, 99.2, 82.7, 73.0, 56.3, 56.2, 42.6.

3-(hydroxy(4-methoxyphenyl)methyl)-5,7-dimethoxyisobenzofuran-1(3H)-one ***(9b)***. White solid, Yield: 73.3%, MP:202.3-203.5^{o}C. ^{1}H NMR (400 MHz, DMSO-d_6) δ 7.25 (d, J = 8.0 Hz, 2H), 6.87 (d, J = 8.0 Hz, 2H), 6.54 (s, 1H), 6.24 (s, 1H), 5.89 (d, J = 4.0 Hz, 1H), 5.54 (d, J = 4.0 Hz, 1H), 4.97 (t, J = 4.0 Hz, 1H), 3.82 (s, 3H), 3.77 (s, 3H), 3.73 (s, 3H). ^{13}C NMR (101 MHz, $CDCl_3$) δ 166.1, 159.5, 151.2, 130.4, 127.8, 113.8, 99.4, 99.3, 82.5, 73.4, 71.48 (s), 55.9, 55.8, 55.3, 42.6. ESI MS (*m/z*) 353 (M+Na); HRMS (ESI) (*m/z*) calcd for $C_{18}H_{18}O_6Na$, 353.0996, found, 353.1004.

3-((4-ethoxyphenyl)(hydroxy)methyl)-5,7-dimethoxyisobenzofuran-1(3H)-one ***(9c)***. White solid, Yield: 64.4%, MP:154.1-154.8 ^{o}C.^{1}H NMR (600 MHz, DMSO-d_6) δ 7.21 (d, J = 12.0 Hz, 2H), 6.83 (d, J = 12.0 Hz, 2H), 6.51 (s, 1H), 6.21 (s, 1H), 5.85 (d, J = 6.0 Hz, 1H), 5.50 (s, 1H), 4.94 (t, J = 6.0 Hz, 1H), 3.98-3.95 (q, J = 6.0, 2H), 3.79 (s, 3H), 3.75 (s, 3H), 1.28 (t, J = 6.0 Hz, 3H). ^{13}C NMR (101 MHz, $CDCl_3$) δ 168.1, 166.1, 159.4, 159.0 (s), 151.1, 130.0, 127.7, 114. 5, 107.6, 99.3, 82.4, 73.6, 63.5, 55.9, 55.8, 14.8. ESI MS (*m/z*) 345 ($M+H^+$); HRMS (ESI) (*m/z*) calcd for $C_{19}H_{21}O_6$, 345.1333, found, 345.1361.

3-(hydroxy(4-propoxyphenyl)methyl)-5,7-dimethoxyisobenzofuran-1(3H)-one ***(9d)***. White solid, Yield: 62.6%, MP:148.6-149.5 ^{o}C. ^{1}H NMR (600 MHz, DMSO-d_6) δ 7.22 (d, J = 6.0 Hz, 2H), 6.84 (d, J = 12.0 Hz, 2H), 6.52 (s, 1H), 6.23 (s, 1H), 5.83 (d, J = 6.0 Hz, 1H), 5.51 (d, J = 6.0 Hz, 1H), 4.93 (t, J = 6.0 Hz, 1H), 3.88 (t, J = 6.0 Hz, 2H), 3.80 (s, 3H), 3.76 (s, 3H), 1.72-1.66 (m, 2H), 0.95 (t, J = 6.0 Hz, 3H). ^{13}C NMR

(101 MHz, $CDCl_3$) δ 168.2, 166.1, 159.4, 159.2, 151.1, 130.0, 127.7, 114.5, 107.6, 99.3, 82.5, 73.6, 69.61 (s), 55.9, 55.8, 22.6, 10.5. ESI MS (*m/z*) 381 ($M+H^+$); HRMS (ESI) (*m/z*) calcd for $C_{21}H_{23}O_6$, 381.1309, found, 381.1337.

3-((4-butoxyphenyl)(hydroxy)methyl)-5,7-dimethoxyisobenzofuran-1(3H)-one ***(9e)***. White solid, Yield: 58.9%, MP:205.8-206.4 ^oC. ^1H NMR (600 MHz, DMSO-d_6) δ 7.21 (d, *J* = 6.0 Hz, 2H), 6.84 (d, *J* = 6.0 Hz, 2H), 6.51 (s, 1H), 6.21 (s, 1H), 5.85 (d, *J* = 6.0 Hz, 1H), 5.50 (d, *J* = 6.0 Hz, 1H), 4.94 (t, *J* = 6.0 Hz, 1H), 3.91 (t, *J* = 6.0 Hz, 2H), 3.79 (s, 3H), 3.75 (s, 3H), 1.67-1.62 (m, 2H), 1.42-1.36 (m, 2H), 0.90 (t, J = 6.0 Hz, 3H). ^{13}C NMR (101 MHz, $CDCl_3$) δ 168.3, 166.1, 159.4, 159.2, 151.1, 130.0, 127.7, 114.4, 107.6, 99.4, 99.3, 82.5, 73.6, 67.8, 55.9, 55.8, 31.3, 19.2, 13.8. ESI MS (*m/z*) 395 (M+Na); HRMS (ESI) (*m/z*) calcd for $C_{21}H_{23}O_6$, 395.1465., found, 395.1494.

*3-((4-(hexyloxy)phenyl)(hydroxy)methyl)-5,7-dimethoxyisobenzofuran-1(3H)-one (****9f****)*. White solid, Yield: 67.1%, MP:157.6-158.5 ^oC. ^1H NMR (600 MHz, DMSO-d_6) δ 7.21 (d, *J* = 12.0 Hz, 2H), 6.84 (d, *J* = 6.0 Hz, 2H), 6.52 (s, 1H), 6.22 (s, 1H), 5.83 (d, *J* = 6.0 Hz, 1H), 5.50 (s, 1H), 4.93 (t, *J* = 6.0 Hz, 1H), 3.91 (t, *J* = 6.0, 2H), 3.80 (s, 3H), 3.76 (s, 3H), 1.69-1.64 (m, 2H), 1.39-1.37 (m, 2H), 1.29-1.28 (m, 4H), 0.86 (t, *J* = 6.0 Hz, 3H). ^{13}C NMR (101 MHz, $CDCl_3$) δ 168.3, 166.1, 159.4, 159.2, 151.2, 130.0, 127.7, 114.4, 107.6, 99.4, 99.3, 82.5, 73.6, 68.1, 55.9, 55.8, 31.6, 29.2, 25.7, 22.6, 14.0. ESI MS (*m/z*) 401 ($M+H^+$); HRMS (ESI) (*m/z*) calcd for $C_{23}H_{29}O_6$, 401.1959., found, 401.1990.

3-(hydroxy(4-isobutoxyphenyl)methyl)-5,7-dimethoxyisobenzofuran-1(3H)-one ***(9g)***. White solid, Yield: 53.8%, MP:155.5-156.7 ^oC. ^1H NMR (400 MHz, DMSO-d_6) δ 7.24 (d, *J* = 8.0 Hz, 2H), 6.86 (d, *J* = 8.0 Hz, 2H), 6.54 (s, 1H), 6.20 (s, 1H), 5.86 (s, 1H), 5.53 (d, *J* = 4.0 Hz, 1H), 4.95 (s, 1H), 4.39-4.34 (m, 1H), 3.82 (s, 3H), 3.76 (s, 3H), 1.67-.62 (m, 2H), 1.21 (t, *J* = 4.0 Hz, 3H), 0.91 (t, *J* = 8.0 Hz, 3H). ^{13}C NMR (101 MHz, DMSO-d_6) δ 167.1, 165.4, 158.7, 157.1, 151.8, 131.7, 128.2, 114.9, 106.6, 99.6, 98.8, 82.1, 74.0, 72.3, 55.7, 28.5, 19.0, 9.5. ESI MS (m/z) 373 ($M+H^+$); HRMS

(ESI) (m/z) calcd for $C_{21}H_{25}O_6$, 373.1646, found, 373.1675.

*3-(hydroxy(4-(2-methoxyethoxy)phenyl)methyl)-5,7-dimethoxyisobenzofuran-1(3H)-one (**9h**).* White solid, Yield: 66.0%, MP:102.6-103.4 ^{o}C. ^{1}H NMR (600 MHz, DMSO-d_6) δ 7.22 (d, J = 6.0 Hz, 2H), 6.85 (d, J = 12.0 Hz, 2H), 6.51 (s, 1H), 6.21 (s, 1H), 5.86 (d, J = 6.0 Hz, 1H), 5.51 (d, J = 6.0 Hz, 1H), 4.94 (t, J = 6.0, 1H), 4.03 (t, J = 6.0, 2H), 3.79 (s, 3H), 3.75 (s, 3H), 3.61 (t, J = 6.0, 2H), 3.27 (s, 3H). ^{13}C NMR (101 MHz, $CDCl_3$) δ 168.3, 166.1, 159.4, 158.8, 151.1, 132.7, 130.5, 127.7, 114.7, 114.5, 107.6, 99.3, 99.2, 82.5, 73.5, 71.0, 67.3, 59.2, 55.9, 55.8, 40.8, 29.7. ESI MS (*m/z*) 375 ($M+H^+$); HRMS (ESI) (*m/z*) calcd for $C_{20}H_{23}O_7$, 375.1438, found, 375.1471.

*3-(hydroxy(4-(3-methoxypropoxy)phenyl)methyl)-5,7-dimethoxyisobenzofuran-1(3H)-one (**9i**).* White solid, Yield: 66.2%, MP:100.8-103.9 ^{o}C. ^{1}H NMR (600 MHz, DMSO-d_6) δ 7.22 (d, J = 6.0 Hz, 2H), 6.85 (d, J = 6.0 Hz, 2H), 6.52 (s, 1H), 6.22 (s, 1H), 5.83 (d, J = 6.0 Hz, 1H), 5.51 (d, J = 6.0 Hz, 1H), 4.94 (t, J = 6.0 Hz, 1H), 3.97 (t, J = 6.0 Hz, 2H), 3.80 (s, 3H), 3.76 (s, 3H), 3.44 (t, J = 6.0 Hz, 2H), 3.22 (s, 3H), 1.92-1.89 (m, 2H). ^{13}C NMR (101 MHz, $CDCl_3$) δ 168.3, 166.1, 159.4, 158.9, 151.2, 130.4, 127.8, 114.4, 107.6, 99.4, 99.2, 82.6, 73.5, 69.2, 64.9, 58.7, 55.9, 55.8, 29.6. ESI MS (*m/z*) 411 (M+Na); HRMS (ESI) (*m/z*) calcd for $C_{21}H_{25}O_6$, 411.1414, found, 411.1426.

*3-(hydroxy(4-(4-methoxybutoxy)phenyl)methyl)-5,7-dimethoxyisobenzofuran-1(3H)-one (**9j**).* White solid, Yield: 58.8%, MP:179.5-182.4 ^{o}C. ^{1}H NMR (400 MHz, DMSO-d_6) δ 7.23 (d, J = 8.0 Hz, 2H), 6.86 (d, J = 8.0 Hz, 2H), 6.54 (s, 1H), 6.24 (s, 1H), 5.89 (d, J = 4.0 Hz, 1H), 5.54 (d, J = 4.0, 1H), 4.97 (t, J = 4.0 Hz, 1H), 3.95 (t, J = 6.0, 2H), 3.82 (s, 3H), 3.78 (s, 3H), 3.35 (t, J = 4.0, 2H), 3.23 (s, 3H), 1.74-1.69 (m, 2H), 1.66-1.59 (m, 2H). ^{13}C NMR (101 MHz, DMSO) δ 167.1, 165.5, 158.7, 157.9, 151.7, 131.7 , 128.1, 113.6, 106.6, 99.7, 98.7, 82.2, 72.4, 71.5, 67.1, 57.8, 55.8, 55.7, 25.6, 25.5. ESI MS (*m/z*) 425 ($M+H^+$); HRMS (ESI) (*m/z*) calcd for $C_{21}H_{23}O_6$, 425.1571, found, 425.1567.

*3-((4-(2-ethoxyethoxy)phenyl)(hydroxy)methyl)-5,7-dimethoxyisobenzofuran-1(3H)-one (**9k**).* White solid, Yield: 48.5%, MP:192.0-192.7 ^{o}C. ^{1}H NMR (400 MHz, DMSO-d_6) δ 7.24 (d, J = 8.0 Hz, 2H), 6.88 (d, J = 8.0 Hz, 2H), 6.54 (s, 1H), 6.23 (s, 1H), 5.87 (d, J = 4.0 Hz, 1H), 5.53 (d, J = 4.0 Hz, 1H), 4.96 (t, J = 4.0 Hz, 1H), 4.05 (t, J = 4.0, 2H), 3.82 (s, 3H), 3.77 (s, 3H), 3.67 (t, J = 4.0, 2H), 3.51-3.46 (q, J = 4.0 Hz, 2H), 1.12 (t, J = 8.0 Hz, 3H). ^{13}C NMR (101 MHz, DMSO-d_6) δ 167.1, 165.5, 158.7, 157.8, 151.7, 131.9, 128.1, 113.6, 106.6, 99.7, 98.7, 82.2, 72.4, 68.3, 67.0, 65.7, 55.8, 55.7, 15.1. ESI MS (m/z) 389 (M+H^{+}); HRMS (ESI) (m/z) calcd for $C_{21}H_{25}O_7$, 389.1595, found, 389.1625.

*3-(hydroxy(4-(2-phenoxyethoxy)phenyl)methyl)-5,7-dimethoxyisobenzofuran-1(3H)-one (**9l**).* White solid, Yield: 57.4%, MP:96.9-97.3 ^{o}C. ^{1}H NMR (400 MHz, $CDCl_3$) δ 7.34-7.29 (m, 4H), 6.96 (d, J = 8.0 Hz, 5H), 6.40 (s, 1H), 6.03 (s, 1H), 5.48 (d, J = 4.0 Hz, 1H), 5.13 (d, J = 4.0 Hz, 1H), 4.34 (s, 4H), 3.91 (s, 3H), 3.74 (s, 3H). ^{13}C NMR (101 MHz, $CDCl_3$) δ 166.1, 159.3, 158.6, 151.2, 131.0, 129.5, 127.9, 121.2, 114.7, 114.6, 107.50 (s), 99.4, 99.2, 82.6, 73.4, 66.7, 66.4, 55.9, 55.8. ESI MS (*m/z*) 459 (M+Na); HRMS (ESI) (*m/z*) calcd for $C_{25}H_{24}O_7Na$, 459.1414, found, 459.1419.

*3-((4-(but-3-en-1-yloxy)phenyl)(hydroxy)methyl)-5,7-dimethoxyisobenzofuran-1(3H)-one (**9m**).* White solid, Yield: 54.7%, MP:95.2-96.9 ^{o}C. ^{1}H NMR (400 MHz, DMSO-d_6) δ 7.23 (d, J = 8.0 Hz, 2H), 6.86 (d, J = 8.0 Hz, 2H), 6.54 (s, 1H), 6.23 (s, 1H), 5.89-5.82 (m, 2H), 5.53 (d, J = 4.0 Hz, 1H), 5.06-4.94 (m, 3H), 3.94 (t, J = 4.0 Hz, 2H), 3.82 (s, 3H), 3.77 (s, 3H), 2.19-2.14 (m, 2H). ^{13}C NMR (101 MHz, $CDCl_3$) δ 168.3, 166.1, 159.4, 159.0, 151.2, 137.8, 130.3, 127.7, 115.2, 114.4, 107.6, 99.4, 99.2, 82.6, 73.5, 67.2, 55.9, 55.8, 30.1, 28.4. ESI MS (*m/z*) 371 (M+H^{+}); HRMS (ESI) (*m/z*) calcd for $C_{21}H_{23}O_6$, 371.1495, found, 371.1501.

*3-((4-(benzyloxy)phenyl)(hydroxy)methyl)-5,7-dimethoxyisobenzofuran-1(3H)-one (**9n**).* White solid, Yield: 56.8%, ^{1}H NMR (400 MHz, $CDCl_3$) δ 7.81 (d, J = 8.0 Hz, 2H), 7.47-7.34 (m, 5H), 7.02 (d, J = 8.0 Hz, 2H), 6.73 (s, 1H), 6.45 (d, J = 4.0 Hz, 1H), 6.32 (s, 1H), 5.12 (s, 2H), 3.99 (s, 3H), 3.97 (s, 3H). ^{13}C NMR (101 MHz,

DMSO-d_6) δ 167.6, 165.9, 159.2, 158.1, 152.2, 137.6, 132.5, 128.9, 128.6, 128.3, 128.1, 114.5, 107.1, 100.1, 99.2, 82.6, 72.8, 69.5, 56.3, 56.2, 49.1.

*3-((4-((4-fluorobenzyl)oxy)phenyl)(hydroxy)methyl)-5,7-dimethoxyisobenzofuran-1(3 H)-one (**9o**).* White solid, Yield: 69.9%, MP:190.5-191.0 ^{o}C. ^{1}H NMR (600 MHz, DMSO-d_6) δ 7.47 (t, J = 6.0, 2H), 7.24 (d, J = 6.0 Hz, 2H), 7.19 (t, J = 6.0 Hz, 2H), 6.93 (d, J = 12.0 Hz, 2H), 6.52 (s, 1H), 6.21 (s, 1H), 5.85 (s, 1H), 5.73(s, 1H), 5.51 (d, J = 6.0, 1H), 5.05 (s, 2H), 3.80 (s, 3H), 3.74 (s, 3H). ^{13}C NMR (101 MHz, $CDCl_3$) δ 166.1, 159.5, 158.6, 151.1, 13.07, 129.3, 127.8, 115.6, 115.4, 114.9, 107.6, 99.3, 82.3, 73.7, 69.4, 56.0, 55.7. ESI MS (*m/z*) 425 ($M+H^+$); HRMS (ESI) (*m/z*) calcd for $C_{24}H_{22}FO_6$, 425.1395, found, 425.1426.

*3-((4-((4-chlorobenzyl)oxy)phenyl)(hydroxy)methyl)-5,7-dimethoxyisobenzofuran-1(3 H)-one (**9p**).* White solid, Yield: 63.5%, ^{1}H NMR (400 MHz, $CDCl_3$) δ 7.38 (s, 4H), 7.33 (d, J = 8.0 Hz, 2H), 6.98 (d, J = 8.0 Hz, 2H), 6.41 (s, 1H), 6.00 (s, 1H), 5.48 (d, J = 4.0 Hz, 1H), 5.14 (s, 1H), 5.07 (s, 2H), 3.93 (s, 3H), 3.73 (s, 3H). ^{13}C NMR (101 MHz, DMSO-d_6) δ 167.5, 166.0, 159.2, 157.9, 152.2, 136.7, 132.8, 129.9, 128.9, 128.7, 114.6, 100.2, 99.3, 82.6, 72.9, 68.7, 56.3, 56.2.

*3-((4-((4-bromobenzyl)oxy)phenyl)(hydroxy)methyl)-5,7-dimethoxyisobenzofuran-1(3 H)-one (**9q**).* White solid, Yield: 65.5%, ^{1}H NMR (400 MHz, $CDCl_3$) δ 7.54 (d, J = 8.0 Hz, 2H), 7.34-7.33 (m, 4H), 6.98 (d, J = 8.0 Hz, 2H), 6.41 (s, 1H), 6.01 (s, 1H), 5.49 (d, J = 4.0 Hz, 1H), 5.14 (d, J = 4.0 Hz, 1H), 5.06 (s, 2H), 3.94(s, 3H), 3.73 (s, 3H). ^{13}C NMR (101 MHz, DMSO-d_6) δ 167.5, 166.0, 159.2, 157.9, 152.2, 137.1, 132.7, 131.8, 130.2, 128.7, 121.3, 115.7, 115.0, 114.6, 107.1, 100.2, 99.3, 82.6, 72.9, 68.7, 56.3.

*3-(hydroxy(4-((4-methylbenzyl)oxy)phenyl)methyl)-5,7-dimethoxyisobenzofuran-1(3H)-one (**9r**).* White solid, Yield: 58.5%, ^{1}H NMR (400 MHz, $CDCl_3$) δ 7.34-7.31 (m, 4H), 7.21 (d, J = 8.0 Hz, 2H), 6.99 (d, J = 8.0 Hz, 2H), 6.40(s, 1H), 5.96 (s, 1H), 5.47 (d, J = 4.0 Hz, 1H), 5.15 (d, J = 4.0 Hz, 1H), 5.05 (s, 2H), 3.92 (s, 3H), 3.70 (s, 3H),

2.38 (s, 3H). ^{13}C NMR (101 MHz, DMSO-d_6) δ 164.5, 163.4, 159.2, 157.7, 152.2, 143.5 137.5, 134.5, 129.4, 128.2, 119.2, 114.5, 97.2, 69.5, 56.2, 21.2.

*4-((4-((4,6-dimethoxy-3-oxo-1,3-dihydroisobenzofuran-1-yl)(hydroxy)methyl)phenoxy)methyl)benzonitrile (**9s**).* White solid, Yield: 56.6%, ^{1}H NMR (400 MHz, $CDCl_3$) δ 7.70 (d, J = 8.0 Hz, 2H), 7.57 (d, J = 8.0 Hz, 2H), 7.34 (d, J = 8.0 Hz, 2H), 6.96 (d, J = 8.0 Hz, 2H), 6.41 (d, J = 4.0 Hz, 1H), 6.10 (s, 1H), 5.46 (d, J = 8.0 Hz, 1H), 5.15 (s, 2H), 5.09 (d, J = 4.0, 1H), 3.92 (s, 3H), 3.76 (s, 3H). ^{13}C NMR (101 MHz, DMSO-d_6) δ 167.5, 166.0, 159.2, 157.7, 152.2, 143.5, 132.9, 128.7, 128.5, 119.2, 114.6, 110.9, 107.1, 100.2, 99.3, 82.6, 72.9, 68.6, 56.3, 56.2, 40.97-40.40 (m), 40.11 (d, J = 21.2 Hz), 39.72 (d, J = 15.5 Hz), 39.38 (s).

*3-(hydroxy(4-((4-(trifluoromethoxy)benzyl)oxy)phenyl)methyl)-5,7-dimethoxyisobenzo furan-1(3H)-one (**9t**).* White solid, Yield: 54.3%, ^{1}H NMR (400 MHz, $CDCl_3$) δ 7.49 (d, J = 8.0 Hz, 2H), 7.35 (d, J = 8.0 Hz, 2H), 7.26 (d, J = 8.0 Hz, 2H), 6.99 (d, J = 8.0 Hz, 2H), 6.41 (s, 1H), 6.04 (s, 1H), 5.49 (d, J = 4.0 Hz, 1H), 5.14 (d, J = 4.0 Hz, 1H), 5.09 (s, 2H), 3.93 (s, 3H), 3.74 (s, 3H). ^{13}C NMR (101 MHz, DMSO-d_6) δ 167.5, 166.0, 159.2, 157.9, 152.2, 148.3, 137.1, 132.8, 130.0, 128.7, 121.5, 114.5, 107.1, 100.2, 99.3, 82.6, 72.9, 68.6, 56.3, 56.2, 49.1.

*3-((4-((4-(difluoromethoxy)benzyl)oxy)phenyl)(hydroxy)methyl)-5,7-dimethoxyisobenz ofuran-1(3H)-one (**9u**).* White solid, Yield: 59.3%, ^{1}H NMR (400 MHz, $CDCl_3$) δ 7.35-7.31 (m, 5H), 7.22 (d, J = 8.0 Hz, 2H), 7.00 (d, J = 8.0 Hz, 2H), 6.40 (s, 1H), 5.96 (s, 1H), 5.49 (d, J = 4.0 Hz, 1H), 5.16 (d, J = 8.0, 1H), 5.06 (s, 2H), 3.93 (s, 3H), 3.71 (s, 3H). ^{13}C NMR (101 MHz, DMSO-d_6) δ 167.6, 1656.0 (s), 159.2, 158.0, 152.2, 150.9, 134.6, 132.7, 129.9, 128.7, 119.2, 116.8, 114.5, 107.1, 100.2, 99.3, 82.6, 72.9, 68.8, 60.2, 56.5, 56.3, 5.2.

*3-((4-(cyclohexylmethoxy)phenyl)(hydroxy)methyl)-5,7-dimethoxyisobenzofuran-1(3H)-one (**9v**).* White solid, Yield: 52.6%, ^{1}H NMR (400 MHz, $CDCl_3$) δ 7.29 (d, J = 8.0 Hz, 2H), 6.88 (d, J = 8.0 Hz, 2H), 6.38 (s, 1H), 6.00 (d, J = 11.0 Hz, 1H), 5.46-5.42

(m, 1H), 5.12-5.09 (m, 1H), 3.89 (s, 3H), 3.86 (s, 1H), 3.76-3.71 (m, 4H), 1.88-1.70 (m, 5H), 1.32-1.16 (m, 4H), 1.09-1.01 (m, 2H). ^{13}C NMR (101 MHz, DMSO-d_6) δ 162.7, 158.0, 157.8, 140.0, 134.9, 131.3, 130.7, 128.8, 114.7, 113.5, 107.7, 98.2, 73.6, 73.0, 56.3, 55.9, 49.1, 44.9, 37.5, 29.7, 26.5, 25.9, 25.7.

*4.5. General procedure C: Synthesis of compounds **10b**, **10n** and **10o***

The appropriate compound (**9b**, **9n** and **9o**, 1.0 mmol, 1.0 equiv), *p*-TsOH (2.0 mmol, 2.0 equiv) was dissolved in benzene (5 mL). The reaction mixture was then stirred at 60 °C for 6 h. After completion, the solvent was evaporated under reduced pressure. The residue was dissolved in EtOAc, washed twice with water and once with brine. The combined organic layer was dried over Na_2SO_4 and then evaporated under reduced pressure. The product was separated using silica gel column chromatography.

*(Z)-5,7-dimethoxy-3-(4-methoxybenzylidene)isobenzofuran-1(3H)-one (**10b**).* White solid, Yield: 60.5%, ^{1}H NMR (400 MHz, $CDCl_3$) δ 7.81 (d, J = 8.0 Hz, 2H), 6.94 (d, J = 8.0 Hz, 2H), 6.72 (s, 1H), 6.43 (s, 1H), 6.31 (s, 1H), 3.98 (s, 3H), 3.96 (s, 3H), 3.87 (s, 3H). ^{13}C NMR (101 MHz, DMSO-d_6) δ 167.5, 164.1, 159.6, 145.1, 142.9, 131.7, 126.4, 114.9, 106.9, 103.3, 100.7, 96.4, 56.8, 56.5, 55.7.

*(Z)-3-(4-(benzyloxy)benzylidene)-5,7-dimethoxyisobenzofuran-1(3H)-one (**10n**).* White solid, Yield: 66.5%, ^{1}H NMR (400 MHz, $CDCl_3$) δ 7.80 (d, J = 8.0 Hz, 2H), 7.47 (d, J = 8.0 Hz, 2H), 7.42 (t, J = 8.0, 2H), 7.37 (d, J = 8.0 Hz, 1H), 7.02 (d, J = 8.0 Hz, 2H), 6.73 (s, 1H), 6.44 (s, 1H), 6.32 (s, 1H), 5.12 (s, 2H), 3.99 (s, 3H), 3.97 (s, 3H). ^{13}C NMR (101 MHz, DMSO-d_6) δ 167.5, 164.1, 159.5, 158.8, 145.1, 143.0, 137.3, 131.7, 128.9, 128.4, 128.4, 126.6, 115.8, 106.9, 103.3, 100.7, 96.4, 69.7, 56.8, 56.6.

*(Z)-3-(4-((4-fluorobenzyl)oxy)benzylidene)-5,7-dimethoxyisobenzofuran-1(3H)-one (**10o**).* White solid, Yield: 62.8%, ^{1}H NMR (600 MHz, $CDCl_3$) δ 7.79 (d, J = 6.0 Hz, 2H), 7.38 – 7.34 (m, 4H), 6.97 (d, J = 6.0 Hz, 2H), 6.70 (s, 1H), 6.42 (s, 1H), 6.29 (s,

1H), 5.06 (s, 2H), 3.96 (s, 3H), 3.94 (s, 3H). ^{13}C NMR (101 MHz, DMSO-d_6) δ 167.5, 164.1, 159.5, 158.6, 145.0, 143.0, 136.3, 133.0, 131.7, 130.1, 128.9, 126.8, 115.8, 106.8, 103.3, 100.7, 96.4, 68.9, 56.8, 56.6.

4.6 Cell culture

Mouse peritoneal macrophages were purchased from BeNa Culture Collection Company (BeiJing, China). RAW264.7 cells were cultured in DMEM (Hyclone, USA) supplemented with 10% heat-inactivated fetal bovine serum (Biological Industries, Israel) in a humidified 5% CO_2 containing atmosphere at 37°C. The cells grew until they converged to 70-80% before treatment.

4.7 Determination of NO

RAW264.7 cells (7×10^4 cells/well) were seeded into 48-well plate and used for experiments 24 h later. RAW264.7 cells were pretreated with compounds (10 μM) for 1 h, co-treated with LPS (0.5 μg/mL) for 24 h. After 24 h collect cell supernatant for experiment. NO production was measured using Griess Reagent assay (Beyotime). Griess reagent were mixed at a ratio of 1:1, and reacted at room temperature for 15 min. Measurement of absorbance at 450 nm with enzyme reader.

4.8 Cell viability assay (MTT)

RAW264.7 cells (1×10^4 cells/well) were seeded into 96-well plate and used for experiments 24 h later. Compounds (20 μM) treated cell for 24 h. Forty microliters of MTT solution (5 mg/mL, Sigma-Aldrich) was then added and incubated for an additional 4 h. After 4 h, cell culture supernatants were removed and DMSO (150 μL) was added to added into per well for dissolving the resulting crystals. Shaking about 10-15 min and the absorbance at 492 nm was measured by a microplate reader (MQX200, Bio-Tek, USA)

4.9 Western blotting

RAW264.7 cells were seeded into 6-well plate with 2×10^6 cells per well and maintained about 24 h. RAW264.7 cell were pretreated with compound **9o** (0.5, 1, 2 μM) for 1 h, co-treated with LPS (0.5 μg/mL) for 0.5 h or 24h.The cells were lysed in 300 μL RIPA cell lysis buffer (Contains PMSF and phosphatase inhibitors, Beyotime china) and incubated on ice for 30 min. Collecting supernatant by centrifugation. The

same amount of protein was separated by SDS-PAGE and transferred to PVDF membrane (GE Healthcare, Amersham, UK). The blotted membrane incubated with the primary antibodies and allowed to react for an additional 16 h at 4 °C. All antibodies obtain from cell signaling Technology, USA. The membranes incubated with a 1:5000 dilutions of HRP-conjugated secondary antibody (Beyotime Biotech, Nantong, China) for 1h at room temperature. Signals were visualized using ECL system (Thermo Fisher Scientific).

4.10 Determination of ROS level

RAW264.7 cells were seeded into 6-well plate with 1.5×10^6 cells per well and maintained about 24 h. RAW264.7 cells were pretreated with compound **9o** (0.5, 1, 2 μM) for 1 h, co-treated with LPS (0.5 μg/mL) for 6 h. The cells were treated with DCFH-DA (BestBio, China) for 30 min at 37 °C cell incubator, and then wash the cells 3 times with cold serum-free fresh medium or PBS. Finally, according to the manufacturer's instructions, use flow cytometry detecting the intracellular reactive oxygen species and analyze by flowjo software.

4.11 Immunofluorescence

RAW264.7 cells were seeded into on glass coverslip in six well plates, fixed with 4% polyformaldehyde (w/v) for 20 minutes at room temperature, and sealed in TBS containing 0.1% Triton X-100 with 5% BSA for 1 hour. The cells were incubated with a primary antibody. After the washing step, they are dyed with DAPI the images were acquired by inverted fluorescence microscope (Olympus, Tokyo, Japan).

4.12 In vivo experiment

The 50 male SD rats were obtained from Animal Department of Anhui Medical University (China). Rats were kept in room temperature of 22 ± 2°C and humidity of around 60% and under a 12:12 h light-dark cycle. All animal protocols were approved by the Ethics Committee in Animal Experimentation at Anhui Medical University (Hefei, China) following the guidelines for Care and Use of Laboratory Animals. After acclimation for one week, rats were randomly divided into groups with 10 rats in each group, including the Normal group, AA group, Sinomenine (60 mg/kg), compound **9o** L (20 mg/kg) and compound **9o** H (40 mg/kg). Complete Freund's

adjuvant consists of incomplete Freund's adjuvant (sigma, USA) and inactivated BCG vaccine (China) (10 mg/mL). Rat was induced by a single intradermal injection of 0.1 mL CFA and saline. All rats were given intragastric administration once a day. All rats measured the left hind swelling level and weight every three days. Mice were anesthetized and sacrificed after 29 days. The ankle joint was harvested fixed in 4% neutral buffered polyformaldehyde solution, and then decalcified in 10% EDTA. The ankles were cut into 4 mm thick and stained with hematoxylin and eosin (HE) for histopathological examination. The histological image was obtained using 3DHISTECH's Slide Converter (3DHISTECH, Hungary).

4.13 Statistical analysis

Data were expressed as the mean ±SEM. Statistical significance was assessed by one-way ANOVA and Turkish test, and differences between the two groups were examined by SPSS (version 14.0; SPNN Inc., Chicago, IL, USA). $p<0.05$ was considered to be statistically significant. All experiments dates were repeated at least three times.

Supporting Information

The following files are available free. ^{1}H NMR and ^{13}C NMR spectra and HRMS of compounds.

Acknowledgment

This work was supported by the National Natural Science Funding of China (21977001).

References

[1] R. Medzhitov, Origin and physiological roles of inflammation, Nature, 454 (2008) 428-435.

[2] A. Linde, D. Mosier, F. Blecha, T. Melgarejo, Innate immunity and inflammation--New frontiers in comparative cardiovascular pathology, Cardiovascular research, 73 (2007) 26-36.

[3] D.L. Laskin, V.R. Sunil, C.R. Gardner, J.D. Laskin, Macrophages and tissue injury: agents of defense or destruction?, Annual review of pharmacology and toxicology, 51 (2011) 267-288.

[4] P.J. Murray, Macrophage Polarization, Annual review of physiology, 79 (2017) 541-566.

[5] M. Benoit, B. Desnues, Jean-Louis M. Macrophage Polarization in Bacterial Infections. J Immunol. 2008 Sep 15;181(6):3733-9.

[6] I. Tabas, C. K. Glass. Anti-inflammatory therapy in chronic disease: challenges and opportunities. Science,339 (2013):166-72.

[7] W.C. Lin, J.S. Deng, S.S. Huang, S.H. Wu, C.C. Chen, W.R. Lin, H.Y. Lin, G.J. Huang, Anti-Inflammatory Activity of Sanghuangporus sanghuang Mycelium, International journal of molecular sciences, 18 (2017).

[8] S. Akira, K.Takeda. Toll-like receptor signalling. Nat Rev Immunol. 2004 Jul;4(7):499-511.

[9] J.R. Baird, A.M. Monjazeb, O. Shah, H. McGee, W.J. Murphy, M.R. Crittenden, M.J. Gough, Stimulating Innate Immunity to Enhance Radiation Therapy-Induced Tumor Control, International journal of radiation oncology, biology, physics, 99 (2017) 362-373.

[10] A. Aderem, R. J. Ulevitch Toll-like receptors in the induction of the innate immune response. Nature. 2000 Aug 17;406(6797):782-7.

[11] G. L. Zhang and S. Ghosh. Toll-like receptor-mediated NF-kappaB activation: a phylogenetically conserved paradigm in innate immunity. J Clin Invest. 2001 Jan;107(1):13-9.

[12] P. Moi, K. Chan I. Asunis, A. Cao, Yuet Wai Kan. Isolation of NF-E2-related Factor 2 (Nrf2), a NF-E2-like Basic Leucine Zipper Transcriptional Activator That Binds to the Tandem NF-E2/AP1 Repeat of the Beta-Globin Locus Control Region. Proc Natl Acad Sci USA. 1994 Oct 11;91(21):9926-30.

[13] M.C. Jaramillo, D.D. Zhang, The emerging role of the Nrf2-Keap1 signaling pathway in cancer, Genes & development, 27 (2013) 2179-2191.

[14] H.K. Bryan, A. Olayanju, C.E. Goldring, B.K. Park, The Nrf2 cell defence

pathway: Keap1-dependent and -independent mechanisms of regulation, Biochemical pharmacology, 85 (2013) 705-717.

[15] A. Paine, B. Eiz-Vesper, R. Blasczyk, S. Immenschuh, Signaling to heme oxygenase-1 and its anti-inflammatory therapeutic potential, Biochemical pharmacology, 80 (2010) 1895-1903.

[16] N.G. Abraham, A. Kappas, Pharmacological and clinical aspects of heme oxygenase, Pharmacological reviews, 60 (2008) 79-127.

[17] R. Motterlini, R. Foresti. Heme oxygenase-1 as a Target for Drug Discovery.Antioxid Redox Signal. 20(2014):1810-26.

[18] J. Wu, J. Ling, X. Wang, T. Li, J. Liu, Y. Lai, H. Ji, S. Peng, J. Tian, Y. Zhang, Discovery of a potential anti-ischemic stroke agent: 3-pentylbenzo[c]thiophen-1(3H)-one, Journal of medicinal chemistry, 55 (2012) 7173-7181.

[19] X. Zou, X.J. Yang, Y.M. Gan, D.L. Liu, C. Chen, W. Duan, J.R. Du, Neuroprotective Effect of Phthalide Derivative CD21 against Ischemic Brain Injury:Involvement of MSR1 Mediated DAMP peroxiredoxin1 Clearance and TLR4 Signaling Inhibition, Journal of neuroimmune pharmacology: the official journal of the Society on NeuroImmune Pharmacology, (2020).

[20] T. Uto, N.H. Tung, R. Taniyama, T. Miyanowaki, O. Morinaga, Y. Shoyama, Anti-inflammatory Activity of Constituents Isolated from Aerial Part of Angelica acutiloba Kitagawa, Phytotherapy research : PTR, 29 (2015) 1956-1963.

[21] L. Liu, Z. Q. Ning, S. Shan, K. Zhang, T. Deng, X. P. Lu,Y. Y. Cheng, Phthalide Lactones From Ligusticum Chuanxiong Inhibit Lipopolysaccharide-Induced TNF-alpha Production and TNF-alpha-mediated NF-kappaB Activation, 71(2005):808-13.

[22] W. Lei, Y.F. Deng, X.Y. Hu, J.N. Ni, M. Jiang, G. Bai, Phthalides, senkyunolide A and ligustilide, show immunomodulatory effect in improving atherosclerosis, through inhibiting AP-1 and NF-kappaB expression, Biomedicine & pharmacotherapy, 117 (2019) 109074.

[23] M. Del-Angel, A. Nieto, T. Ramirez-Apan, G. Delgado, Anti-inflammatory effect

of natural and semi-synthetic phthalides, European journal of pharmacology, 752 (2015) 40-48.

[24] E.S. Choi, J.J. Yoon, B.H. Han, D.H. Jeong, Y.J. Lee, D.G. Kang, H.S. Lee, Ligustilide attenuates vascular inflammation and activates Nrf2/HO-1 induction and, NO synthesis in HUVECs, Phytomedicine : international journal of phytotherapy and phytopharmacology, 38 (2018) 12-23.

[25] H. Guo, L. Sun, S. Ling, J.W. Xu, Levistilide A Ameliorates NLRP3 Expression Involving the Syk-p38/JNK Pathway and Peripheral Obliterans in Rats, Mediators of inflammation, 2018 (2018) 7304096.

[26] W.S. Lee, J.S. Shin, D.S. Jang, K.T. Lee, Cnidilide, an alkylphthalide isolated from the roots of Cnidium officinale, suppresses LPS-induced NO, PGE2, IL-1beta, IL-6 and TNF-alpha production by AP-1 and NF-kappaB inactivation in RAW 264.7 macrophages, International immunopharmacology, 40 (2016) 146-155.

[27] H. J. Ni, H. J. Cheng, W. W. Ge, M. X. Lin, Q. S. Li and B. F. Ruan, Formamide Derivatives of Resveratrol: Synthesis, Characterization and Cytotoxicity, Letters in Drug Design & Discovery, 13(2016) 495-504.

[28] Z. W. Wang, S. B. Li, A Convenient and Stereospecific Synthesis of (Z)-Benzylidenephthalides, Chinese Chemical Letters Vol. 12(2001)955 – 956.

[29] M. watanabe, S. jichi, H. morimoto, K. Nogamiand, S. furukawa. Wittig-horner reaction of dimethyl phthalate 3-phosphonates with aldehydes: Synthesis of 3-ylidenephthalides and characterization of their E- AND Z-ISOMERS. HETEROCYCLES, Vol. 36, No. 3,1993.

[30] L.Z. Chen, W.W. Sun, L. Bo, J.Q. Wang, C. Xiu, W.J. Tang, J.B. Shi, H.P. Zhou, X.H. Liu, New arylpyrazoline-coumarins: Synthesis and anti-inflammatory activity, European journal of medicinal chemistry, 138 (2017) 170-181.

[31] G. Nagy, J.M. Clark, E.I. Buzas, C.L. Gorman, A.P. Cope, Nitric oxide, chronic inflammation and autoimmunity, Immunology letters, 111 (2007) 1-5.

[32] M. Mittal, M.R. Siddiqui, K. Tran, S.P. Reddy, A.B. Malik, Reactive oxygen species in inflammation and tissue injury, Antioxidants & redox signaling, 20 (2014) 1126-1167.

[33] J. Ren, D. Su, L. Li, H. Cai, M. Zhang, J. Zhai, M. Li, X. Wu, K. Hu, Anti-inflammatory effects of Aureusidin in LPS-stimulated RAW264.7 macrophages via suppressing NF-kappaB and activating ROS- and MAPKs-dependent Nrf2/HO-1 signaling pathways, Toxicology and applied pharmacology, 387 (2020) 114846.

[34] A. El-Kenawi, B. Ruffell, Inflammation, ROS, and Mutagenesis, Cancer cell, 32 (2017) 727-729.

[35] A.R. Fetoni, F. Paciello, R. Rolesi, G. Paludetti, D. Troiani, Targeting dysregulation of redox homeostasis in noise-induced hearing loss: Oxidative stress and ROS signaling, Free radical biology & medicine, 135 (2019) 46-59.

[36] Y. Liu, Y. Lu, O. Celiku, A. Li, Q. Wu, Y. Zhou, C. Yang, Targeting IDH1-Mutated Malignancies with NRF2 Blockade, Journal of the National Cancer Institute, 111 (2019) 1033-1041.

[37] W. Li, T.O. Khor, C. Xu, G. Shen, W.S. Jeong, S. Yu, A.N. Kong, Activation of Nrf2-antioxidant signaling attenuates NFkappaB-inflammatory response and elicits apoptosis, Biochemical pharmacology, 76 (2008) 1485-1489.

[38] A. Cuadrado, Z. Martín-Moldes, J.P. Ye, Isabel Lastres-Becker. Transcription Factors NRF2 and NF-κB Are Coordinated Effectors of the Rho Family, GTP-binding Protein RAC1 During Inflammation. J Biol Chem, 289(2014):15244-58.

[39] Z. Liu, L. Tang, H. Zhu, T. Xu, C. Qiu, S. Zheng, Y. Gu, J. Feng, Y. Zhang, G. Liang, Design, Synthesis, and Structure-Activity Relationship Study of Novel Indole-2-carboxamide Derivatives as Anti-inflammatory Agents for the Treatment of Sepsis, Journal of medicinal chemistry, 59 (2016) 4637-4650.

[40] R. Li, L. Cai, D.Y. Ren, X.F. Xie, C.M. Hu, J. Li, Therapeutic effect of 7, 3'-dimethoxy hesperetin on adjuvant arthritis in rats through inhibiting JAK2-STAT3 signal pathway, International immunopharmacology, 14 (2012) 157-163.

[41] R. Li, L. Cai, J. Ding, C.M. Hu, T.N. Wu, X.Y. Hu, Inhibition of hedgehog signal pathway by cyclopamine attenuates inflammation and articular cartilage damage in rats with adjuvant-induced arthritis, The Journal of pharmacy and pharmacology, 67 (2015) 963-971.

Figure Captions

Table 1. Inhibition rates and IC_{50} values of compounds

Figure 1. Structures of some phthalide derivatives with anti-inflammatory activity

Figure 2. Structures of Series **A~C**

Figure 3. Proposed mechanism for the synthesis of compound **9b**

Figure 4. DIAMOND drawing of compound **9b**

Figure 5. Preliminary screening cytotoxic evaluation and inhibition of NO production

Figure 6. Inhibition of the Cytokine Production production

Figure 7. Treatment with LPS induced the accumulation of ROS in RAW264.7 cells.

Figure 8. Effects of compounds **9o** on Nrf2/HO-1 pathway in RAW264.7 cells.

Figure 9. Compound **9o** inhibits LPS-induced activation of NF-κB and MAPKs

Figure 10. Therapeutic effect of compound **9o** on AA rats

Figure 11. Proposed mechanisms for anti-inflammatory action of compound **9o**

Scheme 1. Synthesis of compounds **5a~5e**

Scheme 2. Synthesis of compounds **9a~9v**

Scheme 3. Synthesis of compounds **10b,10n,10o**

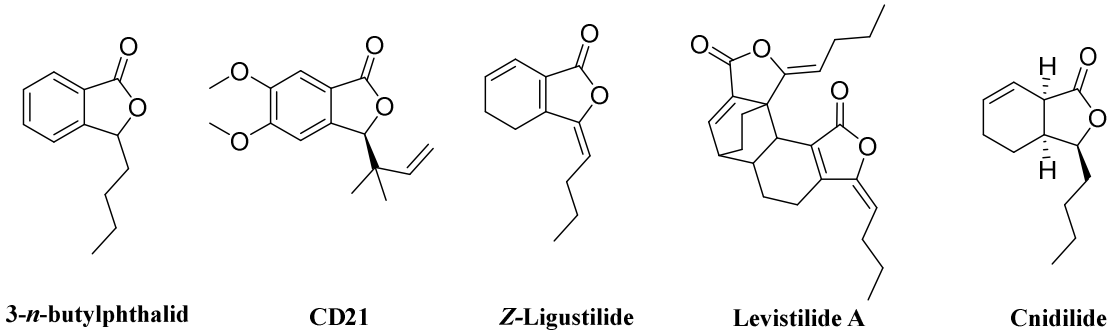

Figure 1. Structures of some phthalide derivatives with anti-inflammatory activity

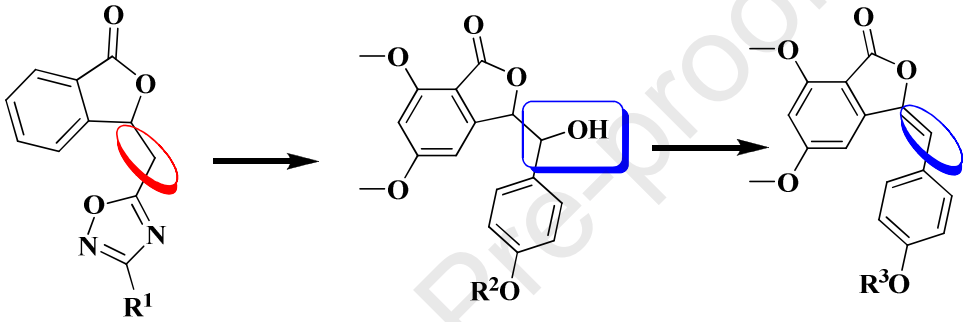

Figure 2. Structures of Series **A~C**

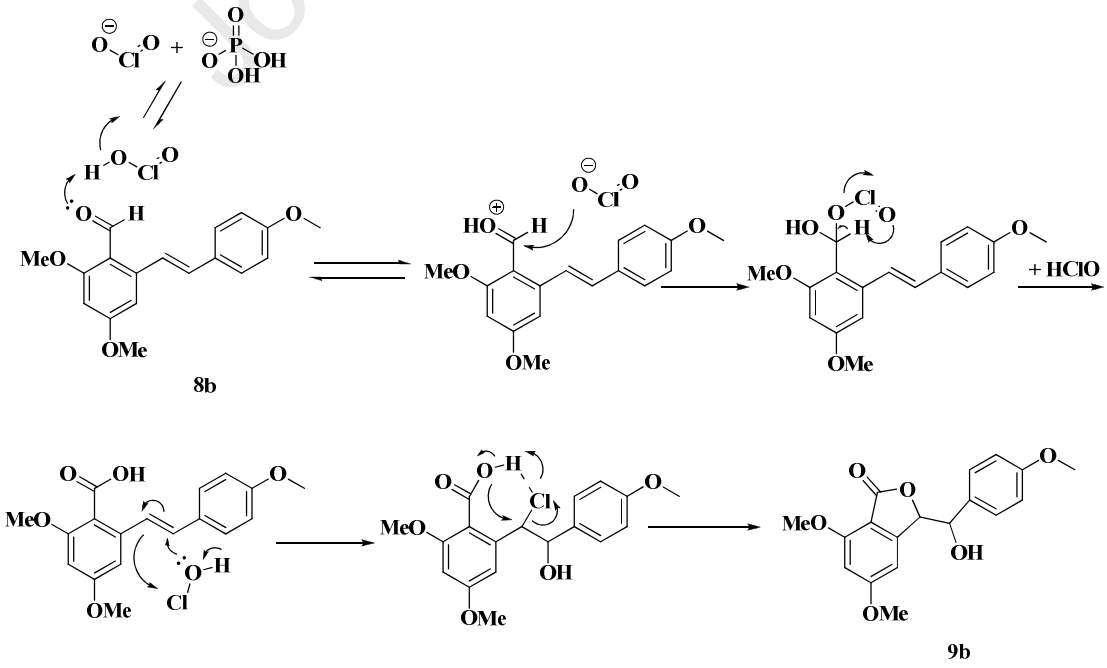

Figure 3. Proposed mechanism for the synthesis of compound **9b**

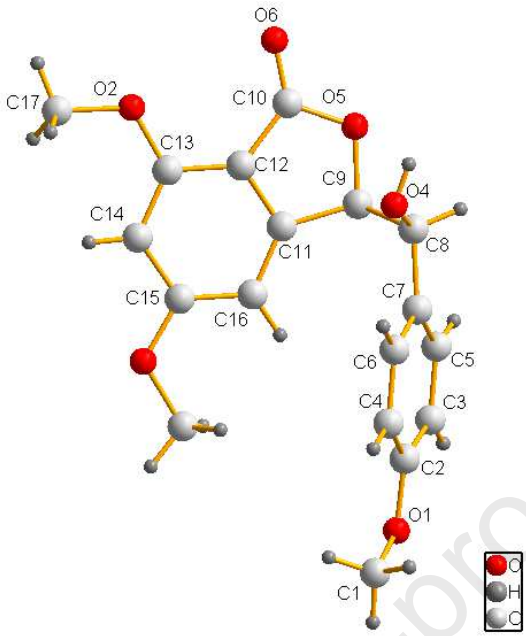

Figure 4. DIAMOND drawing of compound **9b**

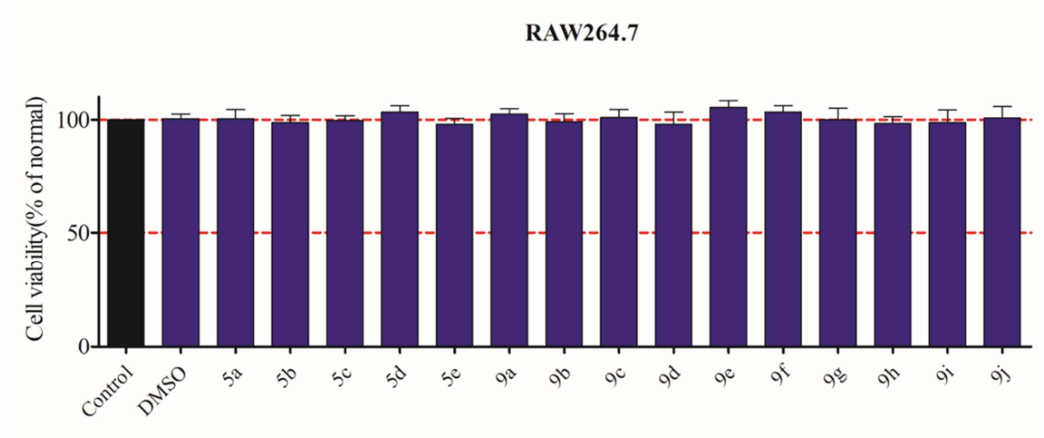

A

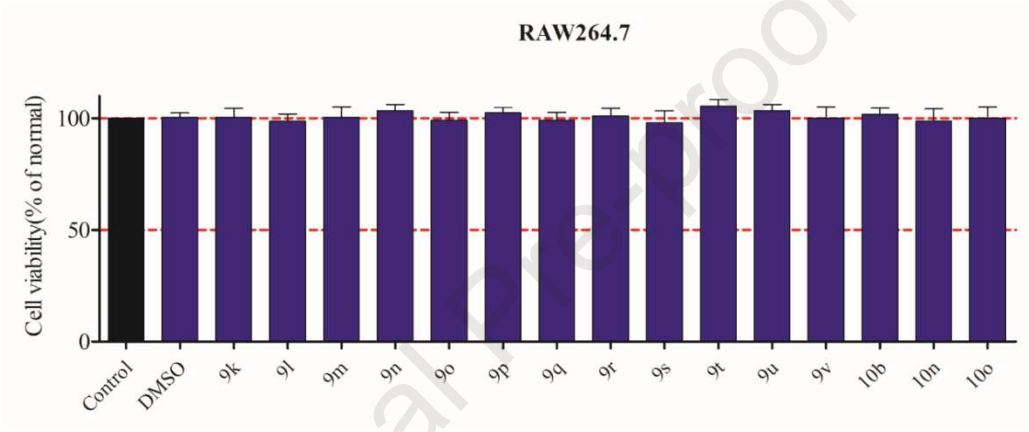

B

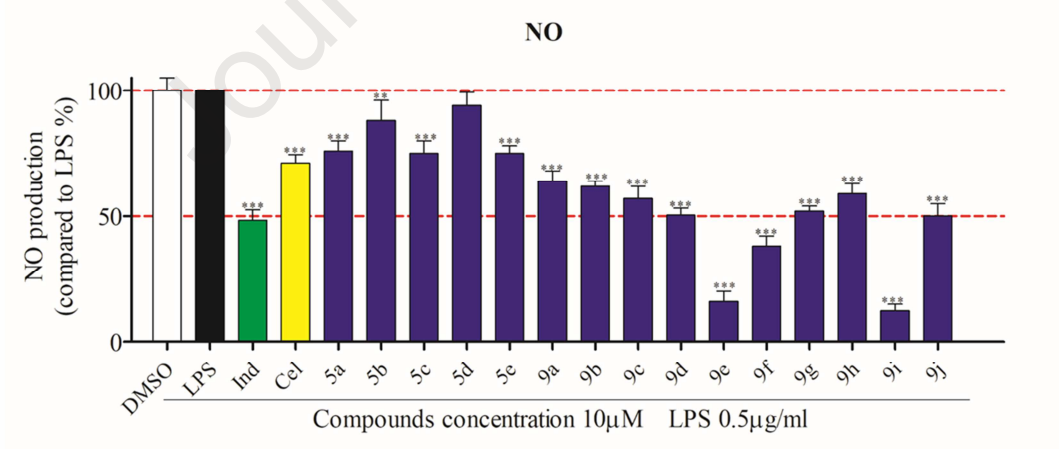

C

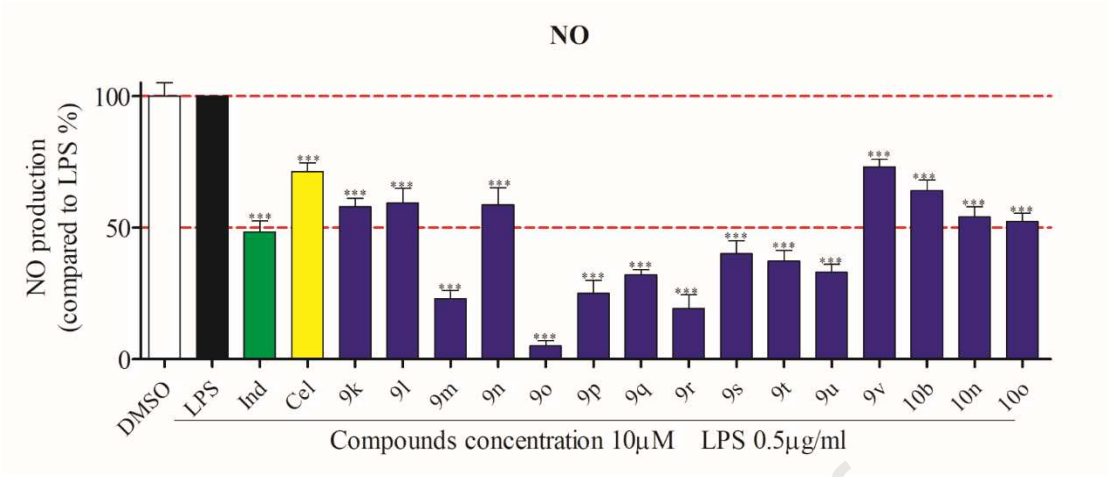

D

Figure 5. Preliminary screening cytotoxic evaluation and inhibition of NO production in RAW264.7 by all compounds. (**A**, **B**) The cytotoxic evaluation in RAW264.7 of compounds **5a~9j** and **9k~10p**. RAW 264.7 cells were pre-incubated with all compounds (20 μM) for 24 h. (**C**, **D**) Inhibition of NO production by all compounds **5a~9j** and **9k~10o.** RAW 264.7 cells were pre-incubated with all compounds (10 μM) for 1 h and treated with LPS (0.5 μg/mL) for 24 h. The concentration of DMSO is 10^{-8} μM. Ind: Positive compound Indomethacin. Cel: Positive compound Celecoxib. ***p<0.001, **p<0.01, *p<0.05 *vs* LPS group.

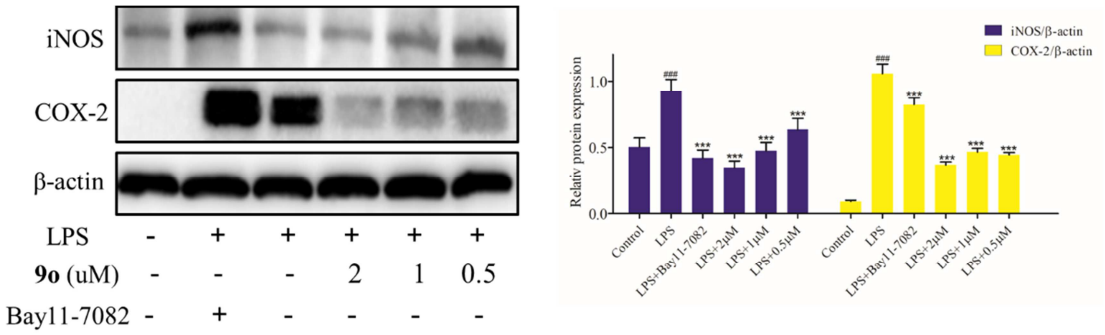

Figure 6. Inhibition of compound **9o** on expression of pro-inflammatory mediators in LPS-stimulated RAW264.7 cells. RAW264.7 cell were pretreated with compound **9o** at concentrations of 0.5, 1, 2 μM for 1 h, incubated with LPS (0.5 μg/mL) for 24 h. iNOS, COX-2 and β-actin were detected by Western blot. Bay11-7082 is the NF-κB inhibitors. $^{###}p<0.001$ compared with Control, $^{***}p<0.001$ compared with LPS-stimulated cells; The blots shown are the examples of three separate experiments.

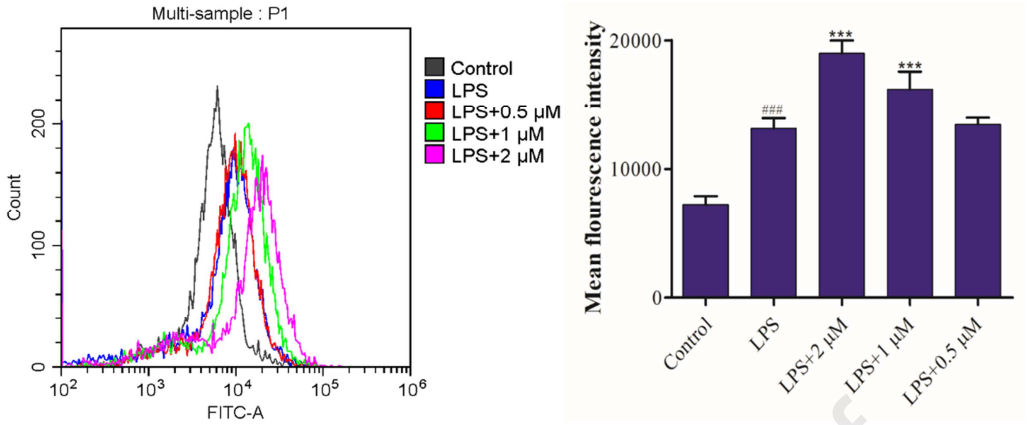

Figure 7. Treatment with LPS induced the accumulation of ROS in RAW264.7 cells. RAW264.7 cells were treated with compound **9o** (0.5, 1 and 2 μM) stimulated with LPS (0.5 μg/mL) for 6 h. The effect of isochromophilone IV on ROS production was studied by analyzing the fluorescence intensity of DCF-DA. $^{###}p<0.001$ compared with the control group; $***p<0.001$ compare with LPS-stimulated cells.

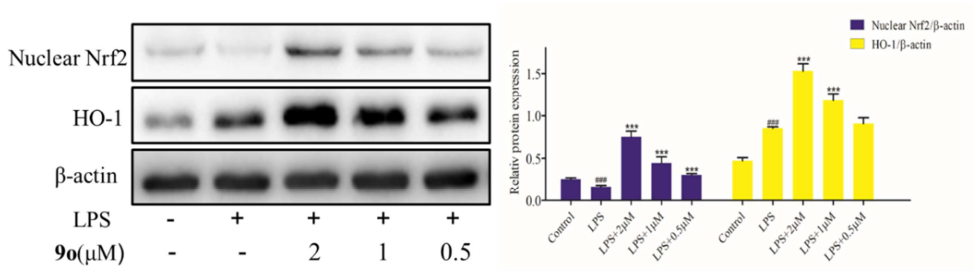

A

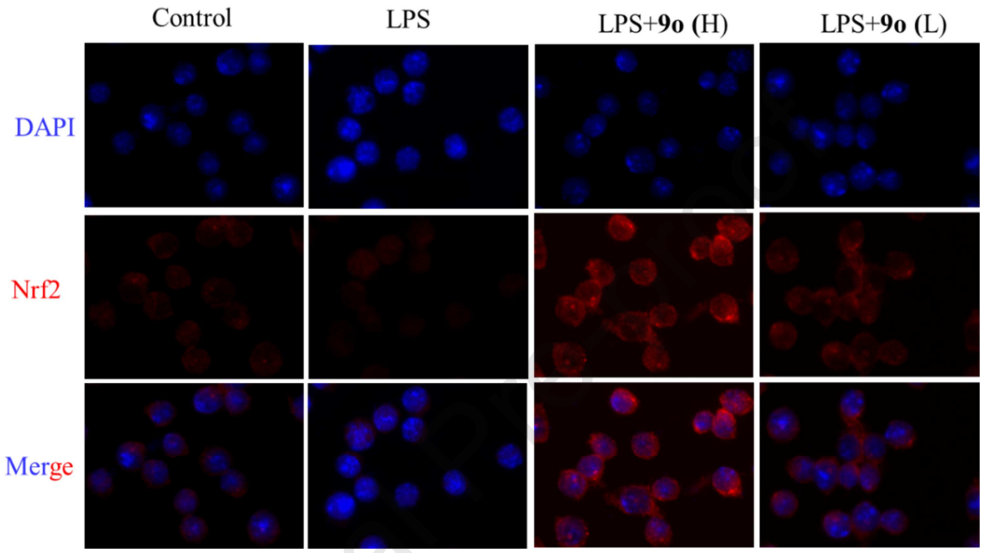

B

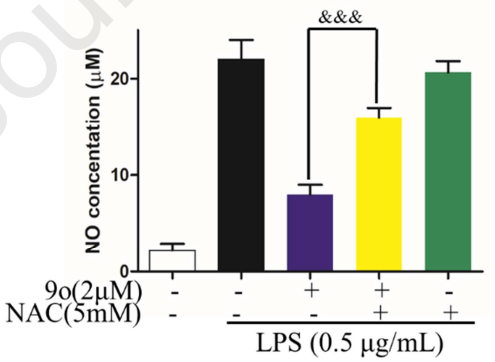

C

Figure 8. Effects of compounds **9o** on Nrf2/HO-1 pathway in RAW264.7 cells. (**A**) Effects of compound **9o** on nuclear Nrf2 and HO-1 protein expression in RAW264.7 cells. RAW264.7 cells were treated with compound **9o** (0.5, 1 and 2 μM) for 1 h, incubated with LPS (0.5 μg/mL) for 24 h. Protein samples of RAW264.7 cells were analyzed by Western blot using anti-Nrf2 antibody and anti-HO-1 antibody. β-actin

was used as the internal control for normalization. (B) Effect of compound **9o** on immunofluorescence subcellular localization of Nrf2 protein in RAW264.7 cells. RAW264.7 cells were treated with compound **9o** for 1 h, incubated with LPS (0.5 μg/mL) for 6 h. Fixed cells were incubated with anti-Nrf2 antibody and FITC-conjugated anti-rabbit IgG antibody, then nuclei were stained with DEPI and observed by fluorescence microscopy. (C) Effect of compound **9o** on NO production in presence of NAC. Cells were pretreated with or without NAC (5 mM) for 1 h in presence of 2 μM compound **9o**, then treated with LPS (0.5 μg/mL) for another 24 h. The culture medium was collected to detect the concentration of NO by Griess reagent. Data shown are the means ± SD from three independent experiments, $^{###}p<0.001$ compared with LPS unstimulated cells, $***p<0.001$ compared with LPS-stimulated cells, $^{\&\&\&}$ $p<0.001$ *vs* NAC plus.

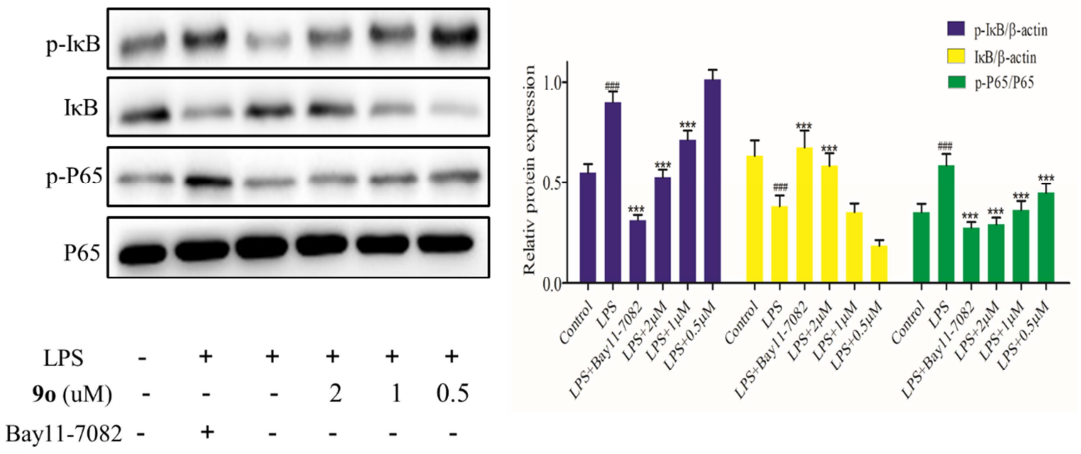

A

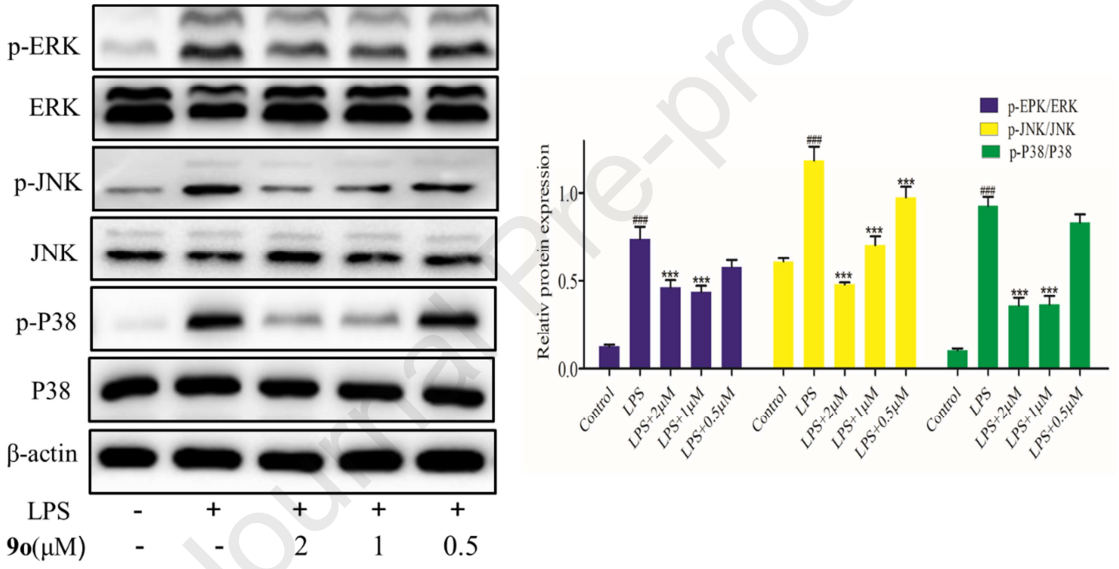

B

Figure 9. Compound **9o** inhibits LPS-induced activation of NF-κB and MAPKs

(**A**) Compound **9o** inhibiter NF-κB signaling pathway in RAW 264.7 cells. (**B**) Compound **9o** inhibiter LPS-induced activation of MAPK signaling pathway in RAW 264.7 cells. After pretreatment with compound **9o** (0.5~2 μM) 1 h, RAW 264.7 cells were stimulated with LPS (0.5 μg/mL) for 30 min. P-IKB IKB, p-P65, P65, ERK, JNK, p38, p-ERK, p-JNK, p-P38and *β*-actin were detected by Western blot. Bay11-7082 is the NF-κB inhibitors. TAK-242 is the MAPK inhibitors. $^{###}p<0.001$ compared with LPS control cells, ***$p<0.001$ compared with LPS-stimulated cells.

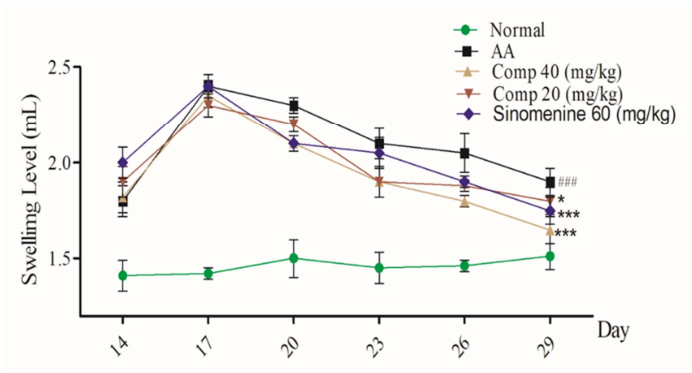

A

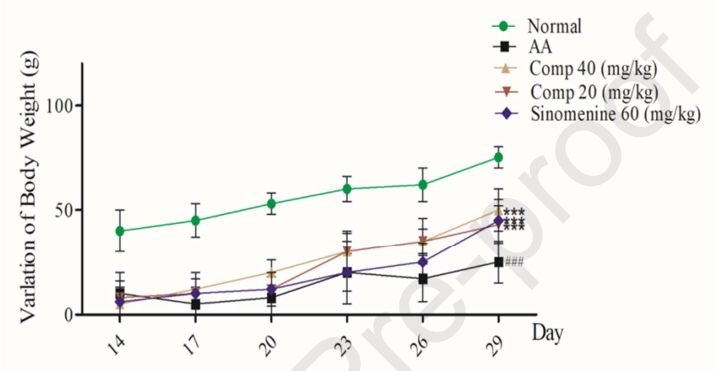

B

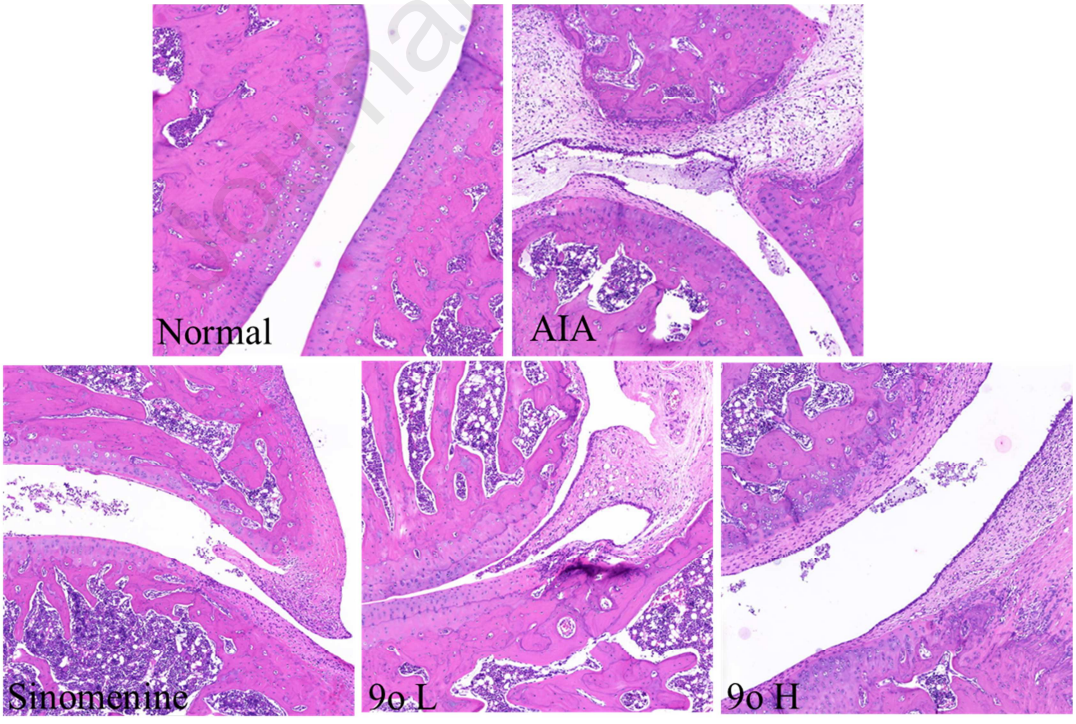

C

Figure 10. Therapeutic effect of compound **9o** on AA rats. **(A)** Effect of compound **9o** on paw swelling of adjuvant arthritis rats; (**B**) Effect of compound **9o** on variation of

body weight in rats. (**C**) Typical histopathological images of ankle joint: (compound **9o** L) compound **9o** 20 mg/kg; (compound **9o** H) compound **9o**, 40 mg/kg; Sinomenine, 60 mg/kg. Sinomenine was the positive control. $^{\#\#\#}p < 0.01$ compared with Normal; $***p < 0.001$, $*p < 0.05$ vs AA group.

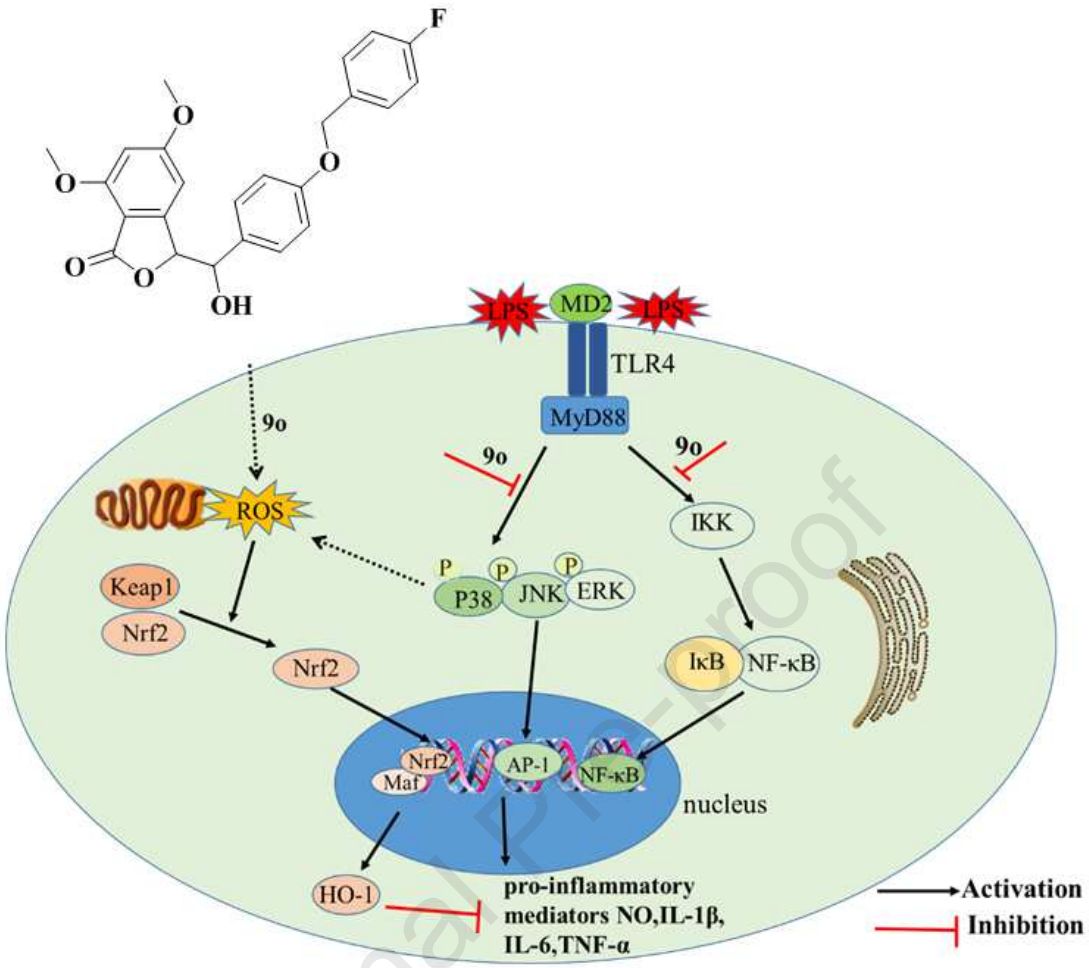

Figure 11. Proposed mechanisms for anti-inflammatory action of compound **9o**

Table1. Inhibition rates and IC_{50} value of compounds

Compd	10 μM (Inhibition rate %)	NO IC_{50} (μM)	cytotoxicity IC_{50} (μM) without LPS	with LPS
5a	24.32±5.34	>10	>40	>40
5b	12.98±4.19	>10	>40	>40
5c	25.12±2.45	>10	>40	>40
5d	10.03±5.12	>10	>40	>40
5e	25.16±3.21	>10	>40	>40
9a	46.12±4.69	>10	>40	>40
9b	38.67±2.35	>10	>40	>40
9c	43.25±3.62	>10	>40	>40
9d	53.21±3.12	9.26	>40	>40
9e	83.67±4.56	1.8	>40	>40
9f	62.24±3.26	5.36	>40	>40
9g	48.65±3.12	>10	>40	>40
9h	41.39±4.01	>10	>40	>40
9i	89.53±4.12	1.26	>40	>40
9j	50.32±2.34	8.21	>40	>40
9k	42.89±3.69	>10	>40	>40
9l	41.23±3.45	>10	>40	>40
9m	87.21±2.36	1.33	>40	>40
9n	41.23±3.59	>10	>40	>40
9o	95.23±3.14	0.76	>40	>40
9p	75.14±4.02	4.32	>40	>40
9q	68.12±5.91	6.53	>40	>40
9r	82.09±3.21	3.12	>40	>40
9s	60.78±2.85	7.36	>40	>40
9t	62.84±4.62	8.14	>40	>40

9u	67.64±4.32	5.03	>40	>40
9v	27.36±3.69	>10	>40	>40
10b	36.28±4.12	>10	>40	>40
10n	44.32±3.78	>10	>40	>40
10o	48.23±3.25	>10	>40	>40
Indomethacin	61.59±1.87%	>10	>40	>40

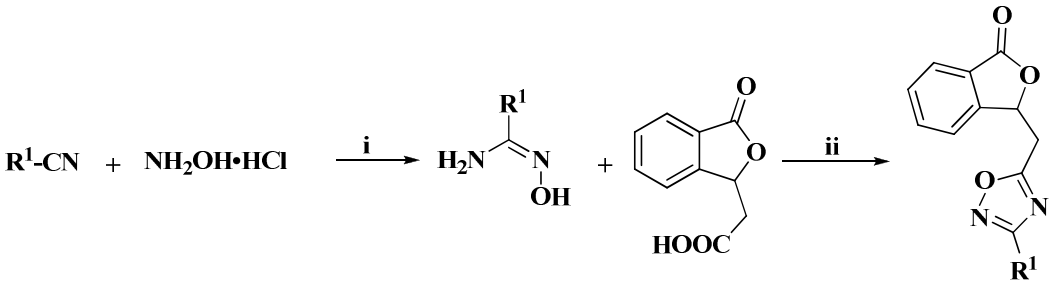

1a-1e **2** **3a-3e** **4** **5a-5e**

5a: **R**^{1}=-CH_3; **5b:** **R**^{1}=-C_6H_5; **5c:** **R**^{1}=-$CH_2C_6H_5$; **5d:** **R**^{1}=-$C_6H_4OC_6H_5$; **5e:** **R**^{1}=-$C_6H_4C_6H_5$

Scheme 1. Synthesis of phthalide-1,2,4-oxadiazole (Series A)

Reagents and conditions: (**iii**) **R**^{2}CH_2Br, K_2CO_3, acetone, reflux, 6 h; (**iv**) DMF, $POCl_3$, CH_3CN, 0 °C to rt, 2 h; (**v**) DMSO, aq. $NaClO_2$, aq. NaH_2PO_4, 50 ^{o}C, 6 h.

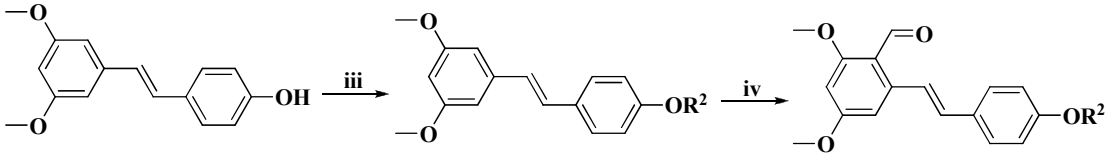

6 **7a-7v** **8a-8v**

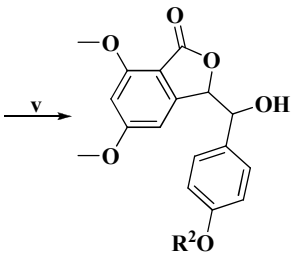

9a-9v

9a: R^2=H; **9b:** R^2= ; **9c:** R^2= ; **9d:** R^2= ; **9e:** R^2= ; **9f:** R^2= ; **9g:** R^2= ; **9h:** R^2= ; **9i:** R^2= ; **9j:** R^2= ; **9k:** R^2= ; **9l:** R^2= ; **9m:** R^2= ; **9n:** R^2= ; **9o:** R^2= ; **9p:** R^2= ; **9q:** R^2= ; **9r:** R^2= ; **9s:** R^2= ; **9t:** R^2= ; **9u:** R^2= ; **9v:** R^2= ;

Scheme 2. Synthesis of 3-hydroxy-benzhydrolphthalide (Series B)

Reagents and conditions: (**iii**) R^2CH_2Br, K_2CO_3, acetone, reflux, 6 h; (**iv**) DMF, $POCl_3$, CH_3CN, 0 °C to rt, 2 h; (**v**) DMSO, aq. $NaClO_2$, aq. NaH_2PO_4, 50 ^oC, 6 h.

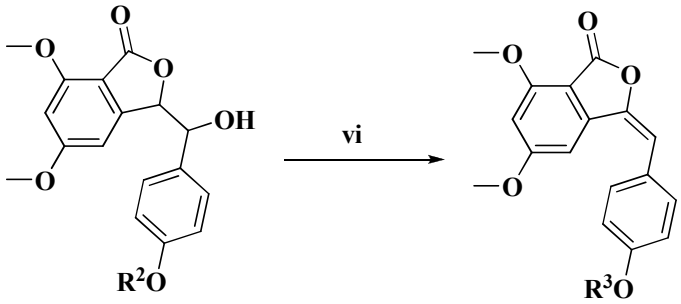

9b, 9n, 9p **10b, 10n, 10p**

10b: R^3=  ; **10n: R^3=**  ; **10p: R^3=** 

Scheme 3. Synthesis of (*Z*)-3-benzylidene-phthalides (Series C)

Reagents and conditions: (**vi**) *p*-TsOH, C_6H_6, reflux, 8 h.

Highlights

► Novel phthalide derivatives were designed and synthesized.

► In *vivo* studies showed that title compound had good therapeutic effect.

► Preliminary mechanisms of anti-inflammatory action were discovered.

Declaration of Interest Statement

Novel phthalide derivatives: synthesis and anti-inflammatory activity *in vitro* and *in vivo*

Liu Zeng Chen[a], Jing Wu[a], Kang Li[a], Qian Qian Wu[a], Rui Chen[a], Xin Hua Liu[a,*], Ban Feng Ruan[*,b]

[a] *School of Pharmacy, Anhui Medical University, Hefei, 230032, P. R. China*

[b] *Key Lab of Biofabrication of Anhui Higher Education, Hefei University, Hefei 230601, P. R. China*

All authors have contributed to the work, have read the manuscript and have agreed to be listed as authors. The submitted manuscript has not been published elsewhere and nor is it currently under review by another publication. No potential conflict of interest relevant to this article.

01/08/2020